A Comparative Study of Fires in Corners and Along Walls

Adam Tegenfeldt & Josef Utterfors

|Avdelningen för Brandteknik | LTH |
LUNDS UNIVERSITET

A Comparative Study of Fires in Corners and Along Walls

Adam Tegenfeldt
Josef Utterfors

Lund 2022

Titel/Title
A Comparative Study of Fires in Corners and Along Walls

Författare/Authors
Adam Tegenfeldt
Josef Utterfors

Report 5685
ISRN: LUTVDG/TVBB--5685--SE

Antal sidor/Number of pages: 63 (including appendices)
Illustrationer/Illustrations: 42

Sökord/Keywords
Fire, wall, corner, hot gas layer, flame height, plume temperature

Abstract
The topic of fires in corners and along walls has been studied previously, however, two different studies conducted in 1987 and 2018 respectively, produced conflicting results regarding plume temperature for fires along walls, as well as hot gas layer temperature for both fires in corners and along walls. This thesis seeks to add data and clarification about fires in corners and along walls.

The work started with a literature review to get clarity on what has already been done in the study of fires in corners and along walls. To add data to the research topic, 12 tests were conducted at the Fire Laboratory at LTH. Using gaseous propane as fuel, a corner-, wall- and centre configuration were used, with heat release rates 5 kW, 10 kW and 20 kW. Another three tests were conducted with the same configurations, but with liquid heptane with a heat release rate of 5 kW. Simulations were run in FDS to replicate some of the tests conducted. The literature review found that there are some differences in the result from different studies.

The results from the experiment were that no differences in the hot gas layer temperature between the wall fires and free-burning fires could be seen, but there was an increase in hot gas layer temperature for corner fires. Plume temperature and flame height for fires in corners and along walls did increase compared to fires in the centre of the room. The simulations in FDS produced results that gave an increase in hot gas layer temperatures for both wall- and corner positions compared to the centre position. Despite being in accordance with theory and previous experiments, the simulations did not produce as high temperatures as predicted.

Brandteknik
Lunds tekniska högskola
Lunds universitet
Box 118
221 00 Lund

www.brand.lth.se
Telefon: 046 - 222 73 60

Division of Fire Safety Engineering
Faculty of Engineering
Lund University
P.O. Box 118
SE-221 00 Lund
Sweden
www.brand.lth.se
Telephone: +46 46 222 73 60

Acknowledgements

We would like to express our deepest appreciation to our supervisor Dr. Nils Johansson, senior lecturer at the Department of Fire Safety Engineering, Lund University, for the support and valuable comments we have received during the thesis.

We would also like to thank Dr. Jonathan Wahlqvist, associate senior lecturer at the Department of Fire Safety Engineering, Lund University, for help with the problems and questions we had surrounding the simulations in FDS.

We are also grateful for the encouraging words and support we have received from our friends and families. This accomplishment would not have been possible without them. Thank you.

Lund 2022

Summary

From previous experiments conducted by McGrattan et al. (2018) and Mowrer and Williamson (1987) the result differed on the impact of a fire placement along a wall regarding the hot gas layer, plume temperature and flame height. This thesis seeks to add data on how wall and corner configurations impact these three parameters and tries to establish what might be the cause of the different results between the two experiments. To achieve this goal, a literature review was performed to establish what previous research had been done in the field, and to add more data an experiment was performed in a small-scale room with different heat release rates.

The literature review resulted in findings from five previous studies that were chosen as important for this thesis. The five different studies presented both similar and different results regarding the chosen parameters. The most important difference being the results on hot gas layer temperature from Mowrer and Williamson (1987) and McGrattan et al. (2018).

The experiment conducted during this thesis was performed in a 1/3 scale of the ISO room with both gaseous propane and liquid heptane as fuel. The heat release rates used were 5 kW, 10 kW and 20 kW. Three positions of the fires were used, corner position, wall position and free-burning fire. For liquid heptane, only 5 kW were tested due to limitations in equipment. The results from the experiment gave results that were different from the experiment by Mowrer and Williamson (1987). No additional temperature increase of the hot gas layer could be attributed to the wall configuration, and despite the hot gas layer temperature being higher from the corner position, the increase was not as high as predicted by Mowrer and Williamson and theory. The MQH modification factors proposed by Mowrer and Williamson for wall and corner configurations did not correspond with the experimental results from this thesis. Flame height was as expected from previous research and experiments increased when placed along the wall and corner compared to the placement in the centre. Calculated flame heights using Heskestads flame height equation did correspond quite well with the visually observed flame heights in the tests with a heat release rate of 5 kW and 10 kW. Plume temperatures increased when the fire was placed along a wall compared to the centre placement and increased even further with a corner configuration.

The cause why the experimental results did not correspond with previous experiments as well as the theory for the hot gas layer temperature might be attributed to several factors. The most likely factor for the difference is that the materials in the compartment had different properties compared to the materials in the study from Mowrer and Williamson (1987). Also, the compartment used for the experiment in this thesis was partially damaged with cracks in walls, ceiling and floor, which might have caused lower temperatures in the hot gas layer when compared to Mowrer and Williamson. The reason why the impact of the wall on the hot gas layer temperatures was small, might be attributed to the flow of air moving the flame away from the wall. The simulations in FDS gave results that agreed fairly well with results from theory and previous studies. However, the simulations did not correspond very well with the experiment conducted within this thesis. The simulations did show an increase in hot gas layer temperature for both the wall and corner configuration, however not as high as predicted in previous studies and theory.

Sammanfattning

Tidigare experiment utförda av McGrattan m. fl. (2018) och Mowrer och Williamson (1987) visade skillnader mellan dessa två i resultatet för brandgaslagrets temperatur, plymtemperatur och flamhöjd för bränder med placering längs vägg. Målet med detta arbete är att tillföra ytterligare data för att öka kunskapen om vägg och hörnpositioners påverkan på plymtemperatur, flamhöjd och brandgaslagrets temperatur, samt vad som kan ha varit orsaken till skillnaden i resultatet från de två experimenten. För att uppnå detta mål genomfördes en litteraturstudie för att undersöka vad som tidigare har gjorts i forskningen om vägg och hörnbränder, dessutom utfördes experiment för att tillföra ytterligare data till forskningen.

Litteraturstudien resulterade i att det hittades fem tidigare studier som var av extra intresse för detta arbete. Dessa fem studier gav både liknande och olika resultat mellan varandra. Främst två av dessa behandlar en brand längs med en vägg och de resulterande parametrar.

Experimentet genomfördes i ett rum med skala 1/3 av ISO-rummet. Som bränsle användes både propan i gasform samt heptan i vätskeform. Effektutvecklingarna som användes var 5 kW, 10 kW samt 20 kW. Tre placeringar av bränder användes, placering i hörn, vid vägg, samt fritt brinnande. För vätskebrand användes endast 5 kW på grund av begränsningar i utrustning. Resultaten av experimentet i detta arbete ligger inte i linje med resultaten som Mowrer och Williamson (1987) kom fram till. Brandgaslagrets temperatur från en brand placeras längst en vägg blev inte högre än från en brand placerad centralt i rummet. Även om branden i hörnet medförde en ökning av brandgaslagrets temperatur, var denna ökning inte lika markant som den från Mowrer och Williamson eller teori. Modifikationsfaktorerna som Mowrer och Williamson tog fram överensstämmer därför dåligt med resultaten från experimentet i detta arbete. I enlighet med tidigare forskning blev flamhöjden som förväntat högre när branden placerades längs väggen i relation till mitten och flamhöjden blev ännu högre på bränder i hörnen. Beräkningar med Heskestads ekvationer för medelflamhöjd för de tre positionerna på bränder passar relativt väl med de visuellt observerade flamhöjderna för 5 kW och 10 kW. Plymtemperaturerna ökade när branden placerades längs väggar och i hörn i relation till en brandplacering i mitten av rummet. Hörnet gav som förväntat högre plymtemperatur än väggen.

Flera olika faktorer tros ha medverkat till skillnaden i resultatet mellan experimentet utfört i detta arbete och tidigare forskning, där skillander i materialegenskaper mellan brandrummet i detta arbete och det brandrum som användes av Mowrer och Williamson (1987) antas vara den mest sannolika faktorn. Rummet som används för experimentet i detta arbete har också tagit skada av tidigare brandförsök, vilket har medfört att sprickor fanns i väggar, tak och golv, vilket kan vara en av anledningarna till de lägre brandgastemperaturerna. En anledning till varför branden längs med väggen ej har en större påverkan kan bero på att inflödet av luft vid flera tillfällen av experimentet flyttat flamman från väggen. Simuleringarna i FDS gav resultat som stämde förhållandevis bra överens med resultat från teori och tidigare forskning, men inte så väl med resultaten från experimentet i detta arbete. Simuleringarna visade på en ökning av brandgastemperaturen för både vägg och hörnbränder, dock var ökningen inte lika markant som visats av tidigare forskning och teori.

Contents

1 Introduction

1.1 Background

During the years that room fires have been studied, the major focus has been on free-burning fires in the centre of a room. Fires which are burning in corners have similarly been studied quite a lot, however, a fire placement flush to a wall has been given less attention compared to free-burning fires and corner fires. From previous experiments conducted by McGrattan et al. (2018) and Mowrer and Williamson (1987) it is known that the placement of a fire flush to a wall or in a corner will affect both the flame height and plume temperature. However, these two experiments seem to differ in their results, as the experiment conducted by McGrattan concluded that the wall had little to no effect on the temperature in the hot gas layer, flame height and plume temperature. Whereas the experiment conducted by Mower and Williamson concluded that the plume temperature, flame height and temperature of the hot gas layer did increase when a fire was placed flush to a wall and that it had to be accounted for in the MQH correlation, which was used to compare the results. Both McGrattan et al. and Mowrer and Williamson used gaseous fuel in their experiments which leaves room to explore the impact of a different fuel source.

The major problem with corner fires and fires along walls occurs indoors. In the years 1998–2021 approximately 10 000 fires in buildings occurred in Sweden each year that required a fire brigade to arrive at the scene. Of those 10 000 fires, approximately 6 000 were fires in residences (MSB, Myndigheten för samhällsskydd och beredskap, 2022). Given how often furniture and other items are placed in corners or close to walls, the significance of the studies conducted on fires in corners and along walls cannot be understated. If there are more studies and research that can prove that the effects of fires in corners and walls create faster and more dangerous fires. As seen with previous research, higher temperatures in the hot gas layer can be predicted to occur in such fires. If studied further, ways to implement building design measures and other countermeasures can be developed, which can limit the impact of the wall and corner effect.

1.2 Purpose and objectives

The purpose of this thesis is to determine how plume temperature, flame height and temperature in the hot gas layer differ when a fire is positioned in a corner, along a wall or in the middle of a room.

The objective of the thesis is to perform an independent experiment on room fires in corners and along walls and determine the impact of the wall and corner on the hot gas layer, flame height and plume temperatures. The thesis will also gather data from previous experiments and studies to establish what has been done previously in the field. Another objective is to determine if a different fuel source will produce different results. One more objective of this thesis is to test whether the modification factors for these correlations can be used to give proper estimates for fires in corners or along walls and if differences are found, suggest possible improvements. Experimental results will be compared with the results from previous sources, hand calculations and simulations that will be made in FDS. The heat release rate will be scaled according to the compartment size used to enable comparison with previous studies.

1.2.1 Problem statement

1. How does a fire along a wall or in a corner impact temperatures in the hot gas layer?

2. How does the calculated result using correlations and the experimental values compare to the results from the experiment?

3. How does the experiment conducted in this thesis compare to previous experiments made?

4. How does a different fuel source affect the results of the experiment?

5. Is it possible to validate simulations using the results from the experiment conducted?

In this thesis, 4 methods will be used and how they will be used is shown in table 1.

Table 1: The methods used to solve the problem statements.

	Method			
Problem statements	Literature-review	Hand-calculations	Experiment	Simulations
1.	X	X	X	X
2.	X	X	X	
3.	X		X	
4.	X	X	X	
5.	X		X	X

1.2.2 Limitations and delimitations

Limitations of this thesis are the number of experiment trials, the compartment size with only one compartment used, and with fibre silicate board and fuel source which is limited to what is available at the fire laboratory at LTH.

The delimitation of this thesis is that it will not seek to identify the limit where the equations are applicable for wall and corner fires. The experimental focus will be on room fires, and not on free-burning fires.

The limitations and delimitation might result in some equations being limited to the compartment size and some equations might not be applicable due to the resulting conditions in the compartment.

2 Theory

In this section relevant theory for fires in corners and along walls, correlations, information and underlying equations for FDS simulations will be presented.

2.1 Theory of fires in corners and along walls

This thesis will only account for turbulent diffusion flames and will not account for laminar or premixed flames as the latter typically do not appear in a normal room fire. It is assumed for the following information from Heskestad (1984), that the surrounding air is uncontaminated by the produced particles from the fire and that it is uniform in temperature (Heskestad, 1984).

Heskestad (1984) describes that for a fire to continue to burn oxygen is needed and in a plume air is entrained across the boundary that is in a figurative way surrounding the flame and extending upwards and confining the entire buoyant flow of entrained air and combustion products. The temperature in the flames lower portions is nearly constant. In the intermittent, upper portion of the flame, the temperature begins to decay due to air entrained and combustion reactions trailing off cooling the flow, see figure 1. Heskestad continues to describe that the maxima of the centreline velocities tend to be located slightly below the mean flame height and that the velocities always decay toward higher elevations, see figure 1. The total heat release rate from a combustion region is either radiated or convected away. The convected heat is carried away by the plume above the flames and the radiated part is the remainder of the heat liberated and is radiated away from the flame in all directions. The radiative fraction tends to decrease with increasing fire size for larger fires. This in turn means that the convective fraction increases and is especially prevalent in fires with smokey hydrocarbons where radiation is increasingly absorbed in the mantle of combustion products surrounding the flames.

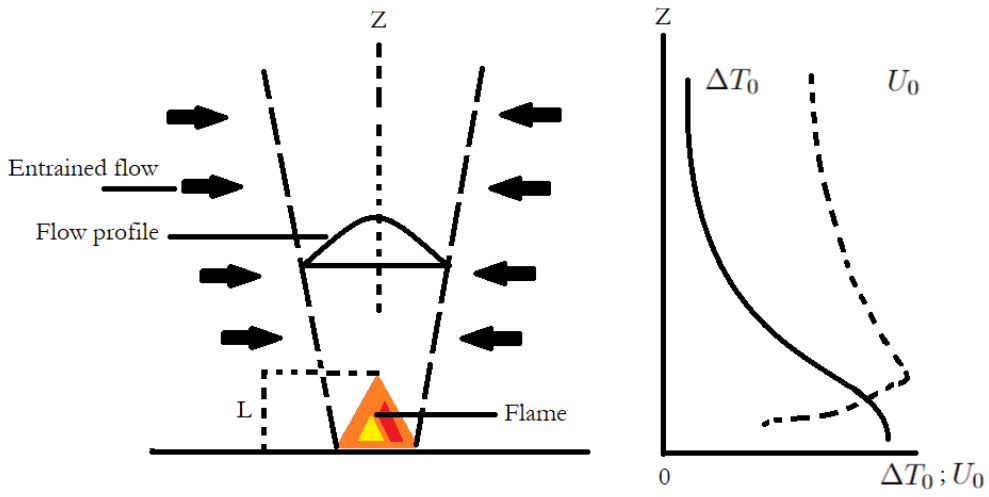

Figure 1: Interpreted representative figure from Heskestad (1984) of temperature and velocities decay with height.

2.1.1 Flame height

To describe flame height or more accurately mean flame height Heskestad (1984) begins with describing how the visible flames above a fire source contain the combustion reactions. In the lower part of the flaming region, the luminosity appears fairly steady. Correspondingly the luminosity of the upper part of the flame appears to be intermittent and sometimes more or less pronounced vortex structures can be observed to form near the base of the flame and shed upwards. The mean flame height L, is the distance above the fire source with an intermittency of 0.5. Intermittency I, decreases to smaller values in the intermittent flame region eventually reaching zero and distance above the fire source z, where $I(z)$ is defined as the fraction of time that at least part of the flame lies above the elevation z. In other words, mean flame height is where the flame lies above the elevation z at least 50 % of the time.

The mean flame height is an important variable that describes where the inert plume can be considered to begin and where combustion reactions are essentially complete. Mean flame heights that are averaged by human eyes tend to be slightly higher than intermittency measurements, (Heskestad, 1984). Other more reliable ways to determine flame height are with the use of digital cameras and software. One such method can be done with the image analysis program to measure flame characteristics, flame tracker (Carmignani, 2021).

Heskestad, 1984 developed equation 1 to calculate mean height as a function of energy release rate and diameter.

$$\mathrm{L} = -1.02\mathrm{D} + 0.235\dot{\mathrm{Q}}^{2/5} \tag{1}$$

Flames in corners and along walls have extended flame heights compared to free-burning flames due to reduced air entrainment as a result of the geometry restriction. For the combustion to access more oxygen the flame height extends to counter the restricted geometry from the wall and corner and the fuel must travel a longer distance to become fully combusted which in turn promotes flame spread by heating walls more effectively (Zeinali, 2019).

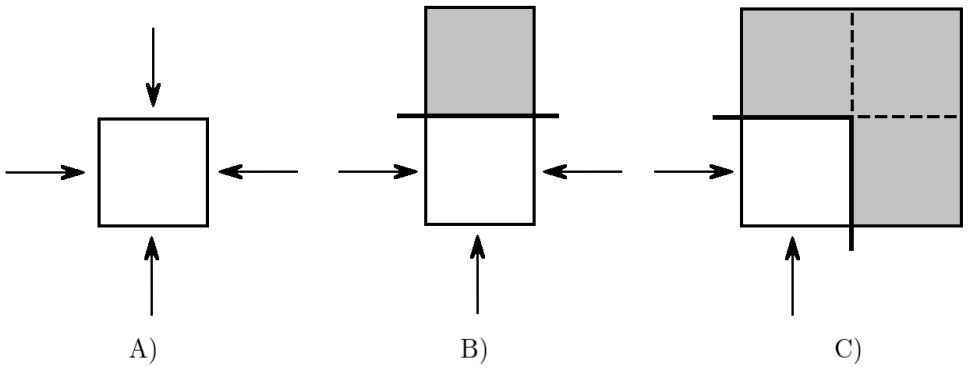

Figure 2: Interpreted figure from Drysdale (2011) and Mowrer and Williamson (1987) of air entrainment (arrows), into a fire A) free burning, B) along a wall and C) in a corner.

As shown in figure 2 a simple model can be used to estimate flame height by using an imaginary mirror image fire source (grey area in the figure). The flame height can be

assumed to be equal to that produced by the actual and imaginary fire sources burning in the open (Drysdale, 2011). Drysdale also states that this concept satisfactorily follows Heskestad's correlation. However, (Hasemi & Tokunaga, 1984) found evidence that the flame height was similar to open burning fires for experimental gas fires in the range $0.4 < \dot{Q}^* < 2.0$. Contrary to the results of Hasemi and Tokunaga, Takahashi et al. (1997) noted from experiments using a square-shaped fire source that the flame height in a corner is almost double provided that the square fire source is placed exactly in the corner and $0.6 < \dot{Q}^* < 4.0$.

By using the aforementioned theory in combination with figure 2 with the assumption that the mass flow from the fire is equal between the white areas, equation 1 can be modified into the following equations for fires in corners and along walls. Where equation 2 is used for walls and equation 3 is used for corners.

$$\mathrm{L} = -1.02(\sqrt{2}\mathrm{D}) + 0.235(2\dot{\mathrm{Q}})^{2/5} \tag{2}$$

$$\mathrm{L} = -1.02(2\mathrm{D}) + 0.235(4\dot{\mathrm{Q}})^{2/5} \tag{3}$$

2.1.2 Plume temperatures

Heskestad (1984) developed the following correlation, equation 4 to estimate the centreline temperature rise $\Delta T_0(x)$ of an plume that is unobstructed at the height z above the firebase. This equation is valid above the flame height.

$$\Delta\mathrm{T}_0(\mathrm{z}) = 9.1\left(\frac{\mathrm{T}_\infty}{\mathrm{g}\mathrm{c}_\mathrm{p}^2\rho_\infty^2}\right)^{1/3}\dot{\mathrm{Q}}_\mathrm{c}^{2/3}\,(\mathrm{z}-\mathrm{z}_0)^{-5/3} \tag{4}$$

where, g is the acceleration of gravity, T_∞ is the ambient temperature, ρ_∞ is the ambient density of air, c_p is the specific heat of air, z_0 is the virtual origin and $\dot{Q}_c$ is the convective heat release rate.

The total heat release rate $\dot{Q}$ is used when calculating the position of the virtual origin and the mean flame height. The convective heat release rate $\dot{Q}_c$ is used when calculating the centreline temperature using equation 4 since this is the part of the energy release rate that causes buoyancy. The total loss of energy from the flames due to radiation is typically between $20\% - 40\%$, with a higher loss for more luminous and sootier flames. The convective heat release rate in building fires is generally between $60\% - 80\%$ of the total energy release rate. Generally, a value of 70% may be assumed without specific knowledge (Heskestad, 1995), therefore $\dot{Q}_c = 0.7\dot{Q}$. The following equation 5 is used to calculate the position of the virtual origin (Heskestad, 1983).

$$\mathrm{z}_0 = 0.083\dot{\mathrm{Q}}^{2/5} - 1.02\mathrm{D} \tag{5}$$

Drysdale (2011) mentions that if a fire is flush to a wall or in a corner the temperatures will be greater due to restriction under the ceiling where the flow is no longer radical and symmetric and due to the lower rate of entrainment into the vertical plume. Drysdale also states that this can be accounted for in equation 4 by multiplying $\dot{Q}_c$ and the area

with a factor 2 for fires along walls and a factor 4 for fires in corners. Modification of the area is modified by multiplying the diameter by $\sqrt{2}$ for fires along walls and 2 for fires in corners.

To calculate the burning rate $\dot{m}''$ (kg/m^{2}s), also referred to as mass loss rate, the following equation, equation 6 can be used (Karlsson & Quintiere, 2022).

$$\dot{\mathrm{Q}} = \mathrm{A_f}\dot{\mathrm{m}}''\chi\Delta\mathrm{H_c} \tag{6}$$

where $\dot{Q}$ is the heat release rate, A_f is the horizontal burning area of the fuel, χ is the combustion efficiency which is the ratio between effective heat of combustion and the complete heat of combustion. For fuels that produce sooty flames, the combustion efficiency is generally around $60\% - 70\%$ and for flames with low visibility that hardly produces any soot the combustion efficiency is close to 100%. ΔH_c is the complete heat of combustion.

The mass loss rate from free-burning pools utilising liquid fuels depends on the diameter and on two empirical constants that are unique to the fuel used and are a function of the radiative heat flux from the flame toward the fuel surface. The following equation 7 can be used to calculate the free burn mass loss rate (Babrauskas, 2016).

$$\dot{\mathrm{m}}'' = \dot{\mathrm{m}}''_{\infty}(1 - \mathrm{e}^{-\mathrm{k}\beta\mathrm{D}}) \tag{7}$$

where k is the extinction-absorption coefficient of the flame, β is the mean beam length corrector and diameter D is assumed to be circular. The data for fuel type is taken from table 26.21 in SFPE (Babrauskas, 2016).

2.1.3 Hot gas layer temperature

One of the correlations for calculating hot gas layer temperatures was developed by McCaffrey, Quintiere and Harkleroad in 1981, commonly referred to as the MQH correlation. Their correlation is based on a simplified energy balance, shown in equation 8, for an upper layer of hot gases with uniform temperature (McCaffrey et al., 1981).

$$\dot{\mathrm{Q}} = \dot{\mathrm{m}}_{\mathrm{g}}\mathrm{c_p}\,(\mathrm{T} - \mathrm{T}_0) + \dot{\mathrm{q}}_{\mathrm{loss}} \tag{8}$$

where $\dot{Q}$ is the heat release rate (kW), $\dot{m}_g$ is the mass flow out of openings (kg/s), c_p is the specific heat of gases (kJ/kgK), T and T_0 is the gas temperature of the upper gas layer and the ambient temperature respectively (K or ℃). Through rewriting, substitution and following a study of a large number of experiments and regression analysis of the results, McCaffrey et al. established the correlation presented in equation 9 (McCaffrey et al., 1981).

$$\frac{\Delta\mathrm{T}}{\mathrm{T_a}} = C_T\left(\frac{\dot{\mathrm{Q}}}{\sqrt{\mathrm{g}}\rho_{\mathrm{a}}\mathrm{c_p}\mathrm{T_a}\mathrm{A_o}\sqrt{\mathrm{H_o}}}\right)^{2/3} \cdot \left(\frac{\mathrm{h_k}\mathrm{A_T}}{\sqrt{\mathrm{g}}\rho_{\mathrm{a}}\mathrm{c_p}\mathrm{A_o}\sqrt{\mathrm{H_o}}}\right)^{-1/3} \tag{9}$$

where ΔT is the temperature difference from the ambient temperature (K or ℃), T_a is the ambient temperature (K), C_T is a correctional factor for temperature, $\dot{Q}$ is the heat

release rate (kW), g is the gravitational constant, ρ_a is the density of the ambient gases (kg/m^3), c_p is the specific heat of the gas (kJ/kgK), A_o is the area of the opening (m^2) and H_o is the height of the opening (m), A_T is the effective surface area (m^2) and h_k is the effective heat transfer coefficient (W/m^{2}K). For C_T McCaffrey et al. (1981) gives a value of 1.63.

h_k in equation 9 can be calculated using the following two equations 10a, 10b.

$$\text{For } t < t_p \qquad h_k = \sqrt{\frac{k\rho c}{t}} \tag{10a}$$

$$\text{and for } t > t_p \qquad h_k = \frac{k}{\delta} \tag{10b}$$

where t_p is the thermal penetration time which indicates the time when $\approx 16\%$ of the temperature increase on the fire-exposed side of an enclosure has reached the back side of the enclosure (McCaffrey et al., 1981).

The MQH correlation is limited by the underlying conditions and assumptions used in the derivation of the method. One assumption is that the gas temperature is uniform in the smoke layer and for conventional-sized rooms, this is a reasonable assumption. Additional limitations are that the rise in temperature must at least be 20 ℃ and at most 600 ℃, however, the temperature limit may be extended upwards somewhat. Another limitation is that the method applies to transient and steady-state fire growths, which means that the heat release rate must be known. MQH assume that the heat is lost due to mass flowing out through openings and because of this the method is only applicable to situations when smoke has started to leave the compartment through openings. The fire cannot be ventilation-controlled and is therefore assumed to be fuel-controlled. The MQH correlation is not applicable for fires flush to walls or in corners without adding modifications factors (Karlsson & Quintiere, 2022).

When a fire is placed flush to a wall or in a corner the MQH correlation needs to be multiplied with a modification factor. Mowrer and Williamson (1987) suggested from both theoretical calculations and after conducting a series of experiments that a modification factor for the entire correlation of 1.7 for fires in corners and 1.3 for fires along walls is appropriate for most opening sizes and shapes of common rooms (Mowrer & Williamson, 1987). However, when reviewed by Foote et al. (1986), it is concluded that the modification factors determined by Mowrer and Williamson actually weaken the performance of the MQH correlation, increasing the standard deviation by 12 K (Deal & Beyler, 1990).

The MQH modification factors were developed using data from compartment fires with a range of window openings and conventional doors, and are therefore not appropriate for use in living areas with an open floor plan (Bruns, 2018).

To determine the maximum heat release rate possible in a certain compartment and if the compartment will result in a fuel controlled- or a ventilation-controlled fire, in relation to the limitations of the MQH method. The assumption is that all the oxygen used for combustion is utilised. This will in turn give a somewhat overestimated heat release rate but it is a good indicator of what is possible in the compartment. Each kilogram of oxygen used for combustion produces approximately 13.2 MJ of energy and

knowing that 23 % of the air mass entering the opening is oxygen the following equation 11 can be used to determine the maximum energy release rate in MW, at ventilation controlled conditions of a compartment (Karlsson & Quintiere, 2022).

$$\dot{Q} = 1.518 \cdot A_0 \sqrt{H_0} \tag{11}$$

2.1.4 Plume mass flow

Experiments were carried out by Zukoski et al. (1980) in which the plume gases from various fires were collected in a hood. In their experiments, the hot gas layer height was kept constant by controlling the flow rate in the hood exhaust. By adjusting the energy release rate and the fuel height the plume mass flow could be defined as a function of both height and energy release rate using several experimental measurements. Zukoski et al. adjusted the ideal plume theory equations to fit the experiments resulting in the following equation, equation 12 (Zukoski et al., 1980).

$$\dot{m}_p = 0.21 \left(\frac{\rho^2 g}{c_p T_a} \right)^{1/3} \dot{Q}^{1/3} z^{5/3} \tag{12}$$

where $\dot{m}_p$ is the plume mass flow in kg/s. Equation 12 is commonly shown in the following form, equation 13 and should preferably be used when the height to the hot gas layer is higher than the flame height.

$$\dot{m}_p = 0.076 \dot{Q}^{1/3} z^{5/3} \tag{13}$$

Another way to calculate plume mass flow is by using Heskestads equation where entrainment into the plume above the flame and into the flame region scale differently. To achieve this the two following equations can be used. Equation 14 when $z > L$ and equation 15 when $z < L$ (Heskestad, 1984).

$$\dot{m}_p = 0.071 \dot{Q}_c^{1/3} (z - z_0)^{5/3} + 1.92 \times 10^{-3} \dot{Q}_c \tag{14}$$

$$\dot{m}_p = 0.0058 \dot{Q}_c \frac{z}{L} \tag{15}$$

Karlsson and Quintiere (2022) describes that one difference between these two equations is that the Zukoski utilises a "top hat" profile across the plume for velocity and temperature and in Heskestad this profile is changed to a more realistic Gaussian profile similar to the flow profile shown in figure 1. Heskestads equation is valid when the flame is in the hot gas layer which should have given better results for the corner configurations.

Mass plume flow for the corner and wall fires have limited access to air entrainment due to the compartment boundaries restricting the possibility of air entraining. Karlsson and Quintiere (2022) reports findings that the air entrainment into the flame follows simple correlations depending on the geometry. The correlation is multiplied either by 1/2 or 1/4 for walls and corners respectively, the same applies to heat release rate, which is multiplied with a factor of 2 and 4 for walls and corners respectively. Equation 16

describes the correlation for a centre-placed fire, and equations 17 and 18 describe the correlation for a wall and corner-placed fire.

$$\dot{m}_p = f(\dot{Q}) \tag{16}$$

$$\dot{m}_p = \frac{1}{2} f(2\dot{Q}) \tag{17}$$

$$\dot{m}_p = \frac{1}{4} f(4\dot{Q}) \tag{18}$$

Zukoski (1995) discusses studies made where fire sources are placed flush against walls or in corners. Studies report that when a burner of circular geometry was placed with one edge tangent to an incombustible wall, little to no influence was noticed on the plume geometry and plume entrainment up to a height of three times the diameter of the burner. When a semi-circular burner was placed in a similar way the plume developed as a half plume with plume properties closely resembling the properties of half the value of a full circular burner of twice the energy release rate. The plume mass flow can then be calculated using equation 17 applied to equation 13, resulting in the following approximation of plume mass flow flush for a wall-placed fire, equation 19.

$$\dot{m}_{p,wall} = 0.048\dot{Q}^{1/3}z^{5/3} \tag{19}$$

Similarly, Zukoski (1995) also reports that for the corner placement the plume mass flow is roughly one-quarter of the flow from the full circular fire with four times the energy release rate, which results in the following approximation of plume mass flow in corners, equation 20.

$$\dot{m}_{p,corner} = 0.03\dot{Q}^{1/3}z^{5/3} \tag{20}$$

Another way to calculate the mass flow out through the opening is by using the following equation, equation 21 from Karlsson and Quintiere (2022), where in stationary conditions $\dot{m}_g$ is equal to $\dot{m}_p$. $\dot{m}_g$ is a combination of the mass flow of rates of cold air entering from the opening and the mass loss rate of the burning fuel. All heights, H_0 are measured from the bottom of the opening and the big difference that distinguishes this method from the well-mixed case is that both the height of the smoke layer, H_D and the height of the neutral plane, H_N is in this case unknown. To solve for this the pressure profile is divided into three parts, the first part of the pressure difference is above the neutral plane where $\dot{m}_g$ flows out. The second part is between the smoke layer and the neutral plane. Here the mass flows into the enclosure but this also happens at the third part of the pressure difference which is located below the smoke layer height. The mass flow rate $\dot{m}_g$ is then achieved by integrating from the height z=0 at the neutral plane up to the height of z = H_0-H_N. This in turn results in the equation, equation 21 (Karlsson & Quintiere, 2022).

$$\dot{m}_g = \frac{2}{3} C_d W \rho_g \cdot \sqrt{\frac{2\,(\rho_a - \rho_g)\,g}{\rho_g}}\,(H_0 - H_N)^{3/2} \tag{21}$$

where C_d is the flow coefficient with a standard value of 0.7 and W is the width of the opening or vent.

The neutral plane is where the pressure difference is zero and the following method can be used to determine the height of the neutral plane needed for equation 21 using experimental data. The pressure and temperature difference at the Bi-directional probe mass flow can be used used to estimate the height to the neutral plane. The general form of the pressure minus the Bernoulli (the hydrostatic pressure difference) can be used, see equation 22.

$$\Delta \mathrm{P}_2 = \Delta \mathrm{P}_1 - (\rho_\mathrm{a} - \rho_\mathrm{g}) \cdot \mathrm{h} \cdot \mathrm{g} \tag{22}$$

Between point 1 and point 2 the average temperature is calculated. The difference in pressure at point 2 can be calculated with the following equation, equation 23

$$\Delta \mathrm{P}_2 = \Delta \mathrm{P}_1 - (\rho_\mathrm{a} - \rho_{\mathrm{g},1\text{–}2}) \cdot \mathrm{h}_{1\text{–}2} \cdot \mathrm{g} \tag{23}$$

where the distance between the two points is h and ρ_g is the average density. The difference in pressure in the points below is calculated by using equation 24

$$\Delta \mathrm{P}_\mathrm{i} = \Delta \mathrm{P}_{\mathrm{i}-1} - (\rho_\mathrm{a} - \rho_{\mathrm{g,i}-(\mathrm{i}-1)}) \cdot \mathrm{h}_{\mathrm{i}-(\mathrm{i}-1)} \cdot \mathrm{g} \tag{24}$$

When ΔP_i switches to a negative value, the neutral plane lies in between point i and point $\mathrm{i}-1$. The height of the neutral plane can then be estimated with linear interpolation.

2.2 Simulation theory

Fire Dynamics Simulator (FDS) is a simulation program developed by National Institute of Standards and Technology (NIST). FDS is basically a CFD program that is designed to specifically simulate fire development.

The code numerically solves the governing Navier-Stoke equations of momentum, mass and energy conservation appropriate for multispecies gas flows with low speed and are thermally driven to describe heat and smoke transport arising from fires (McGrattan et al., 2021b). FDS calculations are performed within a domain made up of rectangular volumes, called a mesh. Each mesh is divided into cells, in which the code is solved. The number of cells in a mesh depends on the desired resolution of the simulation.

To calculate the resolution of the mesh the following equation is used:

$$\mathrm{D}^* = \left(\frac{\dot{\mathrm{Q}}}{\rho_\infty \mathrm{c_p} \mathrm{T}_\infty \sqrt{\mathrm{g}}} \right)^{\frac{2}{5}} \tag{25}$$

D^* is the characteristic diameter of the fire and is in many cases comparable to the fires actual diameter. To calculate the maximum possible cell size δx for the mesh to achieve a certain resolution, the relationship $D^*/\delta x$ is used. The values for mesh resolution should

when possible be between 15–20 (Ma & Quintiere, 2003) but values between 5–10 do for most instances give a satisfying result, with a higher value needed for meshes in closer proximity to the fire (Nystedt & Frantzich, 2011). Nystedt and Frantzich also states that the relative importance of the fire plume's possibility to simulate the transportation of gases depends on the fraction D^*/H, and if $D^*/H < 0.5$, $D^*/\delta x$ should be ≥ 15.

BIV (2013) describes that to simulate the fire as a natural room fire, a dimensionless energy release rate, $\dot{Q}^*$, is used. At high values of $\dot{Q}^*$ the flame acts like a jet flame which in turn means that the momentum of the fuel controls the fire development instead of the gravitation. At low values of $\dot{Q}^*$, there is a risk that the flame breaks up into smaller separate flames. $\dot{Q}^*$ is calculated with equation 26.

$$\dot{\mathrm{Q}}^* = \frac{\dot{\mathrm{Q}}}{\rho_\infty \mathrm{c_p} \mathrm{T}_\infty \sqrt{\mathrm{g}\mathrm{D}}\mathrm{D}^2} \tag{26}$$

According to Cox and Kumar (2002), the value of $\dot{Q}^*$ should be within the interval 0.3–2.5, as this interval represents the natural room fire development. At lower heat release rates combined with larger areas of the fuel source the value of $\dot{Q}^*$ often becomes lower than 0.3. To combat this issue the fire can be divided into smaller fires that activate at designated time intervals so that they together reach the max heat release rate and at the same time minimises the time the fire has a $\dot{Q}^* < 0.3$. Cox and Kumar also states that fires that can be expected to have some momentum of their own, as gas burners do, it can be reasonable to have $\dot{Q}^* > 2.5$. Validation has been made for values of $\dot{Q}^*$ up to 10.6 (McGrattan et al., 2021a) and Hasemi and Tokunaga (1984) states that natural fires always fall into the range $0.1 < \dot{Q}^* < 10$. It can therefore be reasonable to assume that values below 10 are valid.

According to the results of the studies performed by K. Sharma et al. (2010), a reasonable temperature field for the hot gas layer can be obtained when modelling a fire in corners in a test room using the FDS software package. The model used for the study did not incorporate fire spread and the experiments used non-combustible linings. Furthermore, McGrattan et al. (2013) has well-documented the accuracy of FDS when simulating the temperature in the hot gas layer.

3 Literature review

In this chapter literature related to fire in corners and along walls will be presented and compiled to gain an understanding of the differences between studies and experiments which might have caused a difference in the result. These studies that are of interest lay the groundwork for this thesis and will be used to compare the results gathered from this thesis in an attempt to validate if corners and walls do have an effect on primarily the hot gas layer temperature but also plume temperatures and mean flame height. The first pieces of literature were provided by the thesis supervisor in the thesis briefing and these were Mowrer and Williamson (1987) and McGrattan et al. (2018) which were used to start this thesis and to find more relevant literature by finding words and phrases that were unique to this topic and could be used to extend the search.

Sources have been gathered with the help of different search engines. Google was used with its built-in features such as truncation and phrase search to find relevant literature. Google search engine was used in guest mode to avoid getting user-specific results however results unique to the location of the authors might still be prevalent. Truncation and phrase search was also used in LUBsearch which is a collective entry point to all the joint resources in the libraries at Lund University. Additionally, chain search was used to find literature that was referenced in the sources that were relevant to this thesis. The search started wide with relevant words and progressively got more narrow as more relevant words were included. As an example of this, the word fire* was first used with truncation to also search for all abbreviations of the word then to gain more relevant results a phrase search was added for example "hot gas layer" and then add the word "temperature" now the search is fairly relevant and the last word to add is the location of the fire which is highly relevant for this thesis and an example for this might be the word "corner". Trusted and relevant sources are important and where it was possible, the number of citations, publisher, authors and where the studies were found have been used to evaluate the source. A total of five highly relevant articles/publications were found which have been read and summarised in this chapter. The search was conducted between 2022-08-29 and 2022-09-25.

Keywords and key phrases used when searching for relevant literature:

- Fire
- Flame
- Hot gas layer
- Temperature
- Corner
- Wall
- Flame height
- ISO room test
- Wall and corner
- MQH
- Heskestad
- Compartment
- Plume
- Room fire effects
- Smoke layer temperature

3.1 Compiling data from previous studies and experiments

3.1.1 The Influence of Walls, Corners and Enclosures on Fire Plumes, NIST (2018)

McGrattan et al. conducted an experiment in 2018 for NIST in which they used the Heskestad correlation (equation 4) in an attempt to validate the correlation for fires in corners and along walls. They suggested that in order to account for fires along walls and in corners, a simple modification to the correlation would be to increase both the heat release rate ($\dot{Q}$ and $\dot{Q}_c$) and the diameter of the fire (D) with a factor of two and four respectively.

For their experiment, McGrattan et al. (2018) used an enclosure measuring $11.0 \times 7.0 \times 3.8$ m, with walls and ceiling lined with a 13 mm thick gypsum board. An opening of 1.8×2.4 m was placed on the short side furthest away from the corner fire. The floor was covered with 13 mm thick plywood, with the same gypsum boards as used on the walls and ceiling placed on the plywood. The walls and ceiling closest to the areas where the burner was placed were layered with an extra layer of 6 mm thick cement board. The burners were four square natural gas burners, each with the side 30.5 cm, all ganged together. The burners were placed on steel railing to be able to move them away from the wall or corner as the experiment progressed. In total, six tests were made, with heat release rates of 200 kW, 300 kW and 400 kW in a corner, and the same heat release rates against a wall. Each test lasted for 2 hours, with the fire placed flush against the corner or the wall for the first 30 minutes. The fire was then gradually moved away to a distance of 0.1, 0.2, 0.3, 0.5, 1.0 and 1.6 metres from the corner or wall. The first move of the fire took place 30 minutes after the start of the experiment, with a move to the next position made every 15 minutes. For measuring plume temperatures they used 29×3 30 gauge Type K thermocouples placed in a grid at 1.6, 2.2 and 2.9 metres above the burner. They also measured the hot gas layer temperature using thermocouple arrays placed in four vertical trees, placed with the burner in the corner, with the burner at the wall and two additional locations in the enclosure. An approximate sketch of the enclosure used in the experiment is seen in figure 3.

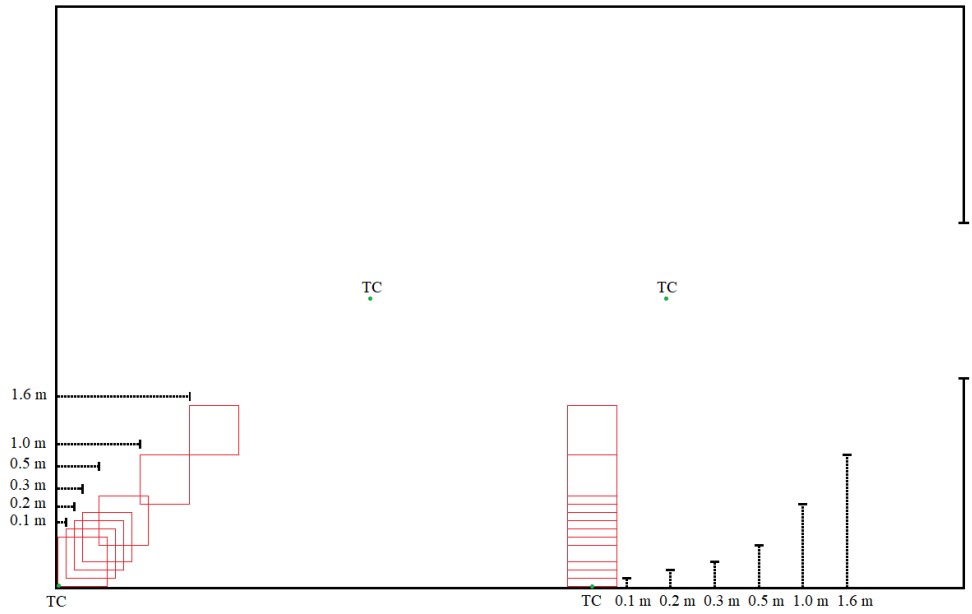

Figure 3: View of the enclosure used by McGrattan et al. (2018). The thermocouple arrays are marked TC.

McGrattan et al. (2018) reported a noticeable effect on flame height and plume temperature for the corner test, with decreasing height and temperature as the fire was moved away from the corner. They did, however, not find any effect on flame height or plume temperature for the wall test as the fire was moved away from the wall. They report that they did not see any effect on the hot gas layer temperature from either corner fires or wall fires, they did however state that the lack of effect on the hot gas layer temperature could be the result of the relatively large compartment. The results they achieved from using the modified Heskestad correlation for fires flush to a corner or wall did for most of the cases overestimate the temperatures when compared with temperatures from the experiments. The percentual deviation from temperatures from experiments when compared to the temperatures calculated by the Heskestad correlation is presented in tables 2, 3, 4 and 5. The values on the left side of the tables are the heights at which the temperatures were measured and calculated. For fires flush in a corner or wall, as seen in tables 2 and 3, the modified Heskestad correlation is used, whereas for fires 1.6 m away from the corner or wall, as seen in tables 4 and 5, no modification was made when using the Heskestad correlation.

Table 2: Corner fires flush in the corner.

	200 kW	300 kW	400 kW
1.6 m	21%	19%	8%
2.2 m	5%	4%	21%
2.9 m	-12%	-17%	-14%

Table 3: Wall fires flush against the wall.

	200 kW	300 kW	400 kW
1.6 m	63%	82%	67%
2.2 m	39%	37%	50%
2.9 m	0%	1%	-6%

Table 4: Corner fires 160 cm from the corner.

	200 kW	300 kW	400 kW
1.6 m	9%	19%	27%
2.2 m	-2%	-5%	-1%
2.9 m	-34%	-30%	-24%

Table 5: Wall fires 160 cm from the wall.

	200 kW	300 kW	400 kW
1.6 m	8%	8%	6%
2.2 m	-14%	-14%	-16%
2.9 m	-38%	-34%	-36%

From the tables above, it is noted that some of the temperatures deviate by a rather large amount, especially for the wall fires. McGrattan et al. (2018) states that no attempt was made to account for the effect of the hot gas layer, which they state could explain some of the differences between the calculated results and the measurements.

3.1.2 Estimating Room Temperatures from Fires along Walls and in Corners, Mowrer & Williamson (1987)

Experiments were conducted by Mowrer and Williamson (1987) to estimate room temperatures from fires along walls and in corners by using experiments and the MQH method, see equation 9. They concluded that a modification factor of 1.3 for fires against walls and 1.7 for fires in corners for the MQH correlation gave an appropriate estimate for the temperature in the hot gas layer. They state that an exception to this modification factor might be the case of ventilation-limited mass flow since it was not studied in the experiment.

The experiments were conducted in a room fire test compartment at the University of California with the dimensions $2.44 \times 3.66 \times 2.44$ m. The room had a single opening for ventilation with dimensions 0.76×2.03 m. The fuel source used for the experiment was a propane-fired, sand-filled diffusion flame burner with dimensions 0.3×0.3 m at a height of 0.3 metres above the floor. The propane burner was adjusted to produce a heat release rate of 40 kW for five minutes followed by an increase of heat release rate to 80 kW for another five minutes and then increased once more to 160 kW for five additional minutes. The compartment was lined with gypsum wall boards for all tests. The experiment had three configurations, with the burner placed in the centre, in a corner and against a sidewall (Mowrer & Williamson, 1987).

The plume theory used by McCaffrey et al. (1981) relates the temperature difference within the plume to the entrainment rate as seen in equation 27.

$$\mathrm{dT_p} \propto \mathrm{Q/m_p} \tag{27}$$

For any given heat release rate (Q), the temperature difference from ambient temperature will vary inversely with the entrainment of air into the plume, as seen for corner fires in equation 28 and for wall fires in equation 29.

$$\frac{\mathrm{dT_{p_{cor}}}}{\mathrm{dT_{p_{cen}}}} = \frac{\mathrm{m_{p_{cen}}}}{\mathrm{m_{p_{cor}}}} \tag{28}$$

$$\frac{\mathrm{dT_{p_{side}}}}{\mathrm{dT_{p_{cen}}}} = \frac{\mathrm{m_{p_{cen}}}}{\mathrm{m_{p_{side}}}} \tag{29}$$

Mowrer and Williamson (1987) predicted mass flows for the standard room fire test compartment for heat release rates of 50–1000 kW. The entrainment ratios they found were in the range of 1.83 for 50 kW to 1.58 for 1000 kW for corner configuration and 1.33 for 50 kW to 1.25 for 1000 kW for wall configuration. As already stated in chapter 2, they chose to select values near mid-range to reduce overall errors, and therefore suggested 1.7 for corner configurations and 1.3 for wall configurations. The temperatures from their experiment are shown in figure 4. The measured temperatures from the experiment and the calculated temperature from the MQH correlation are presented in figures 5, 6 and 7. For the calculated values in figures 5, 6 and 7, a configuration factor of 1.3 and 1.7 was used for wall fires and corner fires respectively, while the correlation was left without modification factor for the centre position fire.

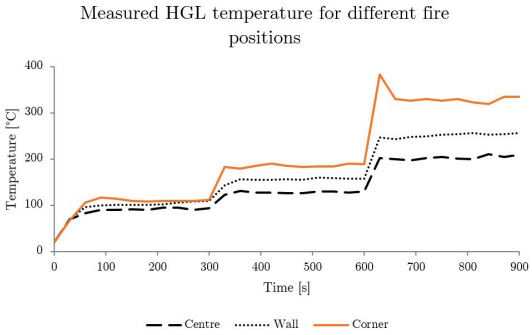

Figure 4: Hot gas layer temperature measured from tests with different fire positions.

The difference in per cent between the temperatures from the tests Mowrer conducted and their calculated values from the MQH correlation were 2.9 % with a standard deviation of 7.7 °C for the centre fire, 0.3 % with a standard deviation of 10.8 °C for the wall fire and 6.1 % with a standard deviation of 17.5 °C for the corner fire. Overall the values from the experiment correspond well with the calculated values from the MQH correlation.

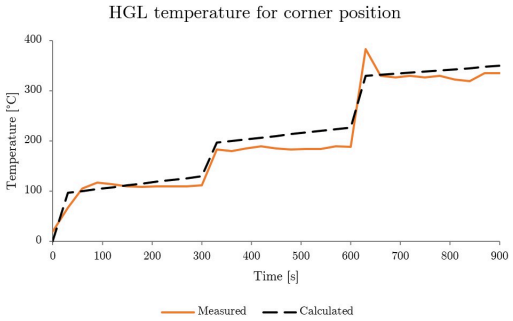

Figure 5: Measured and calculated hot gas layer temperature for corner configuration.

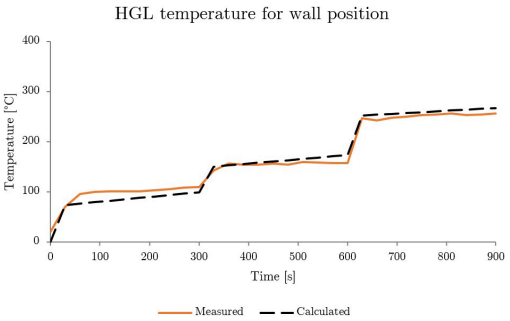

Figure 6: Measured and calculated hot gas layer temperature for wall configuration.

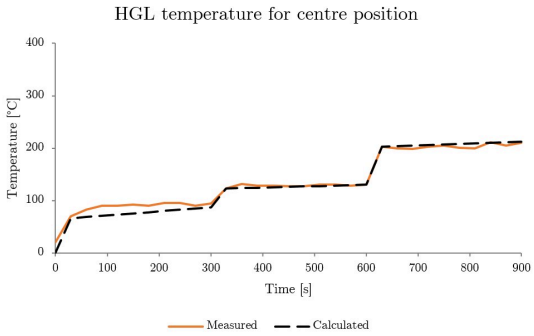

Figure 7: Measured and calculated hot gas layer temperature for centre configuration.

Mowrer and Williamson (1987) concludes that besides the aforementioned modification factors that apply to the ratio of air entrainment that a fire in a corner is equivalent with respect to temperature difference to a fire about twice as large in the centre of a room. This statement is also rewritten by Mowrer and Williamson to describe that a fire in a corner of a room requires about half the heat release rate to cause flashover as opposed to a fire in the centre of a room. As such a wall only requires 70% of the centre heat release rate to cause flashover.

3.1.3 An interrogation of the MQH correlation to describe centre and near corner pool fires, Azhakesan et al. (2003)

Azhakesan et al. (2003) conducted an interrogation of the MQH correlation and the modification factors that Mowrer and Williamson (1987) suggested. Azhakesan et al. (2003) studied previously conducted experiments performed to study the glazing of wall materials in both a full-scale room with measurements $2.4 \times 3.6 \times 2.4$ m and a 1/3 scale room of the same enclosure, with measurements $1.2 \times 0.8 \times 0.8$ m. There was a doorway in each of the rooms, measuring 2×0.8 m and 0.67×0.27 m respectively. For some of the experiments in the full-scale room, half the doorway width was used. Both rooms were lined with low-density Duraboard at the walls and ceiling, however, one of the walls in each experiment was lined with either single or double glazing. The experiments used mineralised industrial methylated spirits as fuel, with HRR of 155 ± 35 kW over 800 s for the full-scale room, and $\sim 14.5 \pm 4.5$ kW for the 1/3 scale room.

For their analysis, Azhakesan et al. (2003) represented the terms in each bracket of equation 9 as a dimensionless variable, $Q_0^{*2/3}$ and $Q_L^{*-1/3}$ respectively. Their calculations resulted in C_T in equation 9 of 2.9 for corner tests with both full and half door width, and C_T of 2.3 for centre fire tests using half door width. Albeit the value of 2.9 is rather close to the original value of 2.8 that Mowrer and Williamson (1987) found in their experiments, the value of 2.3 differs significantly from the value of 1.63 obtained by McCaffrey et al. (1981) for centre fires. Azhakesan et al. do however state that the data from the centre room fire tests were limited to larger fires in the region of 400–600 kW and gas temperatures of ~ 800 °C. The original MQH correlation has an upper limit of 600 °C (McCaffrey et al., 1981). The data from the centre room fire tests were also taken from experiments that utilised half door width, which is another factor that could contribute to the difference in the C_T values.

Azhakesan et al. (2003) states that the C_T value for corner configurations is in accord with the modification factor of 1.7 for the MQH correlation suggested by Mowrer and Williamson (1987).

3.1.4 A CFD Validation of Fire Dynamics Simulator for Corner Fire, CFD Letters (2010)

K. Sharma et al. (2010) performed simulated experiments using FDS and the resulting data was validated with previous results from real fire experiments and by performing a grid sensitivity study. The simulated compartment measured $2.4 \times 3.6 \times 2.4$ m with a door measuring 0.8×2.0 m, ISO test room.

The fire source was placed in a corner and three temperature validation locations were used, near the fire, in the middle of the room and below the door frame. Thermocouples were used to measure the gas temperature. The placement was 0.05 metres below the ceiling centre, 0.1 metres below the top of the door frame and 0.05 metres below the ceiling directly above the burner. Two experiments using plasterboard wall lining materials are considered. This means that there is no fire spread and the heat release rate was only contributed by a methane burner with the dimensions $0.3 \times 0.3 \times 0.3$ m. Two different heat release rates were used in the experiments. For the ISO experiment, experiment A, a heat release rate of 100 kW was used for the first 10 minutes and was after this point increased to 300 kW for an additional 10 minutes. In the other experiment, experiment B, methane was supplied to generate a heat release rate of 40 kW for the first five minutes and was hereafter increased to 160 kW for an additional 10 minutes.

As mentioned previously, FDS was used to calculate the temperature field that was generated by the burner inside the room. No fire spread was incorporated in FDS as the experiments they used to validate the result from the simulation used non-combustible linings on the walls. The walls of the compartment were programmed as heat-conducting media using the conjugate heat transfer approach. To achieve this, the computational domain was made up of the indoor gas domain, with a ceiling that was 0.1 metres thick, 0.1 metres thick walls and 0.1 metres thick floor. The boundary and the computational domain were extended to the exterior wall surface in order to account for the heat transfer into the wall. To eliminate the boundary conditions produced by the doorway plume region, the computational domain was extended by a few centimetres beyond the door. At this location, pressure boundary conditions were applied. To resolve the subscale turbulence resulting from the fire-generated buoyancy-driven flow which is turbulent and results in natural convection, the LES turbulence model was employed. The input for the stable heat release rate was designed to represent the heat release rate in the experiments that were measured with a cone calorimeter. A grid sensitivity was performed, first with 0.1 metres based on the author's previous experience and after that an even finer grid with 0.05 metres cells (K. Sharma et al., 2010).

As mentioned previously in the theory chapter, K. Sharma et al. (2010) concludes that reasonable temperature fields for the hot gas layer can be obtained when modelling a fire in a test room using the FDS software package. The LES turbulence model is suitable to use for the modelling of buoyancy-generated turbulence, as long as the meshing size is sufficient to resolve the subscale turbulence (K. Sharma et al., 2010).

3.1.5 Evaluation of PHOENICS CFD Fire Model Against Room Corner Fire Experiments, Yunlong Liu and Vivek Apte (2004)

Yunlong and Vivek (2004) evaluated the performance of a general-purpose CFD software package named PHOENICS by comparing the temperature field predicted by the software with measurements from room corner fire experiments performed by CSIRO, Fire science and technology laboratory. Similar to the conclusions of K. Sharma et al. (2010) reasonable temperature field can be obtained for the modelling of a fire in a test room using the PHOENICS software package. The computational domain should include the solid wall as the heat conduction into the wall accounted for a large portion of the total heat transfer. This can in turn influence the CFD modelling accuracy of the indoor gas temperature development. If meshing size is sufficient to resolve the subscale turbulence then the $K - \epsilon$ turbulence model is suitable for the modelling of buoyancy-generated turbulence.

The measurements obtained from CSIRO and the experimental method are of interest for this thesis, however, the measurements in the original source Webb et al. (1999) are not available as it is an internal rapport. As such the measurements will be taken from Yunlong and Vivek (2004) which is reliable as the authors had access to the internal report. Additionally, it is worth noting that these measurements are the same that was used to validate the FDS simulations in the previous section, section 3.1.4.

The CSIRO experiment was performed in the ISO test room. Plasterboard wall linings were considered in the experiment resulting in no fire spread. A methane burner was placed in the corner with the dimensions $0.3 \times 0.3 \times 0.3$ m. As mentioned in section 3.1.4 for the ISO test, experiment A, a heat release rate of 100 kW was used for the first 10 minutes and after this point, the HRR was increased to 300 kW for an additional 10 minutes. In the other experiment, experiment B in 3.1.4, methane was supplied to generate a heat release rate of 40 kW for the first five minutes and was hereafter increased to 160 kW for an additional 10 minutes. Gas temperatures were measured with thermocouples placed 0.05 metres below the ceiling centre and 0.1 metres below the centre of the doorway. One thermocouple was also placed 0.05 metres below the ceiling directly above the burner (Yunlong & Vivek, 2004).

The following figures, figure 8, 9 and 10 are a representation of the data presented by Yunlong and Vivek (2004) to describe the results from the experiment performed by CSIRO, Webb et al. (1999).

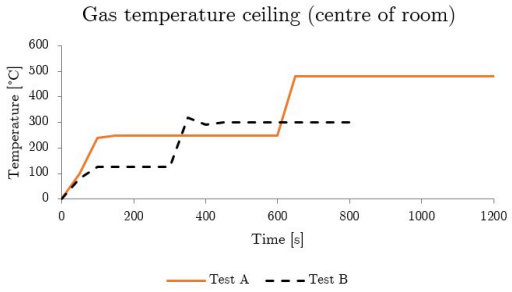

Figure 8: Gas temperature 0.05 metres below the ceiling in the centre of the room in the experiment performed by CSIRO.

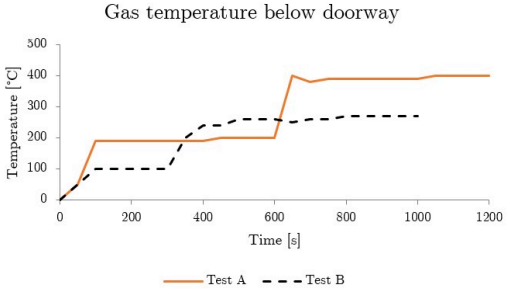

Figure 9: Gas temperature 0.1 metres below the centre of the doorway in the experiment performed by CSIRO.

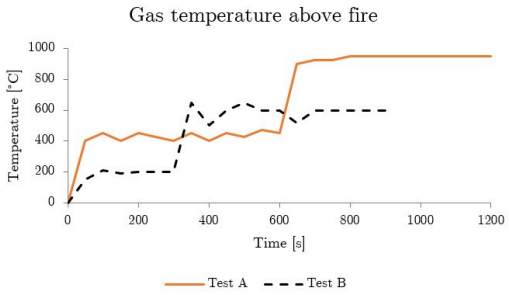

Figure 10: Gas temperature of right above the flame, 0.05 metres below the ceiling in the experiment performed by CSIRO.

4 Method

4.1 Scaling

In order to decide a comparable HRR for the experiment in this thesis, a scaling method was used to compare the HRR used in this thesis with the HRR used in Mowrer and Williamson (1987), K. Sharma et al. (2010) and Yunlong and Vivek (2004), whom all uses the same HRR. When scaled, the HRR for the smaller compartment used in this thesis gives a result that can be compared to the result from experiments with a higher HRR and a larger compartment. Hansen and Ingason (2010) presents correlations for scaling HRR, as seen in equation 30.

$$\dot{Q}_F = \dot{Q}_M \cdot \left(\frac{L_F}{L_M}\right)^{5/2} \tag{30}$$

with the subscripts F and M representing full-scale and model respectively. Only the HRR is scaled, other parameters, such as heat flux, might not be scaled accordingly and could present a source of error in the scaling.

The room used by Mowrer and Williamson (1987) has a scale of 3.05 compared to the room that was used in this thesis. The scaled HRR from the experiment conducted by Mowrer and Williamson is presented in table 6.

Table 6: Downscaled HRR for the small-scale room experiment compared to Mowrer and Williamson (1987).

	Q_1 (kW)	Q_2 (kW)	Q_3 (kW)
Mowrer	40	80	160
Small-scale	2.6	4.9	9.8

As the experiment used to validate the simulations in K. Sharma et al., 2010 and the experiment conducted by Yunlong and Vivek (2004) are the same, these are presented together in table 7 and labelled experiment A and experiment B as in section 3.1.4.

Table 7: Downscaled HRR for the small-scale room experiment compared to experiments A and B from K. Sharma et al. (2010) and Yunlong and Vivek (2004)

	Q_1 (kW)	Q_2 (kW)	Q_3 (kW)	Q_4 (kW)
Experiment A and B	40	160	100	300
Small-scale	2.6	10.3	6.4	19.2

For the experiment conducted by McGrattan et al. (2018), scaling with the dimensions used in this report is not possible since the aspect ratios (L/W and L/H) of the rooms are not the same. The scale of the length is 9.2, the scale of the width is 8.8 and the scale of the height is 4.8. Therefore no scaling was made for this enclosure.

4.2 Experiment

The results from Mowrer and Williamson (1987) and McGrattan et al. (2018) differed regarding the hot gas layer temperature, where Mowrer and Williamson produced results that the hot gas layer temperature did increase with a wall and corner configuration, whereas McGrattan et al. reported results that did not. Another difference between the two is the flame height measured in McGrattan et al., where no difference in flame height could be seen for the wall configuration compared to a free-burning fire, but Mowrer and Williamson producing results with increased flame height for wall configuration compared to a free-burning fire. The two studies had different experimental setups where compartment size, heat release rate and approach to measure the result was different. As there was a conflicting result between the two studies regarding the hot gas layer temperature and flame height for wall configuration when compared to the centre configuration, it was decided to conduct an experiment in order to have more data to analyse and compare with. The experiment was conducted at the Fire laboratory at LTH and took place in a small room setting. Three configurations of fire positions were utilised, free-burning fire, fire in a corner and fire along a wall. Three different heat release rates were used, 5, 10 and 20 kW. 10 and 20 kW were decided from the scaling method used, see tables 6 and 7, to determine how heat release rate in relation to position impacts plume temperature, flame height and temperature in the hot gas layer. The base amount of tests was 9 and repetitions were performed for the wall and corner another day resulting in a total of 15 tests for gas fuel. 3 tests were performed with liquid fuel where repetitions were made another day on all configurations resulting in a total of 6 tests.

A first test was performed before the experiment, with the goal of identifying the influence of the room on the fire with liquid fuel since two different sizes of containers were available. According to calculations, in a free burning scenario, the smaller of the containers with dimensions 0.1×0.1 m would produce around 5 kW and the larger with dimensions 0.18×0.18 m would produce around 27 kW. It is known that pool fires are affected by radiative heat flux from the flame and other surfaces toward the fuel surface (Karlsson & Quintiere, 2022). This means that the compartment was likely to increase the heat release rate and if this happens the smaller container with the measurements 0.1×0.1 m was to be used. The test concluded that the smaller container was to be used and the heat release rate would be approximately 5 kW.

Time was given between each test to allow the compartment to cool down in order to avoid unnecessary heat from walls and ceilings affecting the hot gas layer temperature. A cooling simulation was performed using CFAST simulation with the 1/3 scale ISO-test room dimensions to determine if one-hour tests, 15 minutes of burning and 45 minutes of cooling down the compartment were enough to not impact the next test. The conclusion from the simulation in CFAST was that 45 minutes should be enough to let the compartment cool down. This was also verified with an infrared thermometer during the experiments.

4.2.1 Fuel

For the tests with gaseous fuel, propane (C_3H_8) were used and for the tests with liquid fuel, heptane (C_7H_{16}) were used. These fuels were chosen as those are the fuel available at the fire laboratory.

To achieve the desired mass loss rate required for the predetermined heat release rate for the gas fuel, equation 6 was used to solve for $\dot{m}''$. This mass flow rate or burning rate was converted by using the area of the burner into a flow of litres per second then adjusted into the flow meter on the gas burner to gain the desired heat release rate. The same process to calculate the mass loss rate was performed for the liquid fuel with the addition of equation 7 to calculate the free burn mass loss rate.

4.2.2 Equipment

For the experiment, a 1/3 scale of the ISO-test room (small-scale room), with dimensions $1.2 \times 0.8 \times 0.8$ m and an opening measuring 0.267×0.667 m on one of the short sides was used, see figure 11. The room was made of fibre silicate boards with a thickness of 0.03 m. For the gas fire, a burner with dimensions $0.1 \times 0.1 \times 0.1$ m was used and placed on a 2 cm high metal block for the corner and wall fires to stabilise the burner, see figure 12. For the fire with a liquid fuel source a square container with dimensions $0.1 \times 0.1 \times 0.06$ m was used, see figure 13. The container was filled with 2 dm^3 of water to gain a higher flame base. For the wall and corner tests, the liquid fuel container was placed on two slices of fibre silicate board to gain stability. Two thermocouple trees were used. One thermocouple tree was placed in the opposite corner from the placement of the burner, see figure 15. A figure of the thermocouple tree can be seen in figure 14. There were seven thermocouples in the thermocouple tree, at heights 0.15, 0.32, 0.44, 0.50, 0.56, 0.62, 0.74 and 0.78 m above the floor. Four more thermocouples were placed just below the door frame together with the pressure sensors, at heights 0.46, 0.51, 0.56 and 0.61 m above the floor. A handheld thermocouple was used to measure the plume temperature. A problem can occur when using thermocouples as the thermocouple measure its internal temperature. The internal temperature is affected by the surrounding temperature, but also incoming radiative heat flux, which disturbs the accuracy of the measurement of the surrounding temperature.

Figure 11: 1/3 scale of ISO room under a hood for smoke gas extraction.

Figure 12: Gas burner filled with sand.

Figure 13: Container for liquid fuel with water to get a higher flame base.

Figure 14: Thermocouple tree.

Figure 15: Thermocouple tree in the right corner of the room.

4.2.3 Safety

To minimise the probability and consequence of hazards involved in the experiment a simplified risk analysis was performed before the thesis. Safety equipment and certain safety procedures were utilised. Safety goggles, safety gloves and safety clothes lowered the consequences. Goggles minimised the risk of liquid spilling into the eyes. Gloves protected against the potentially high temperatures in the container after a test even though the container had been left to cool off between tests. Clothes were used to protect against leakage and spillage of liquid fuel. A fire extinguisher was close by to minimise the risk of fire spreading outside of the test compartment and to protect in the event of a leakage of liquid that has been ignited. To prevent gas leakage when the flow had been started, a flame was placed above the gas burner to get ignition. Gas flow was slowly raised to the desired flow to achieve our predetermined heat release rates. Caution was practised when moving the container with liquid fuel to minimise the risk of leakage and the liquid was not ignited until the container was in the desired position. After the experiment was complete, the container was not moved until it has cooled down. This was also to ensure that any remaining fuel will be burned away to lower the risk of leakage.

4.2.4 Procedure

Ventilation-controlled fire calculation using equation 11 was used to determine if the chosen heat release rates for the experiment were too high and if the fire would be fuel controlled as intended. For the small-scale ISO room, the maximum heat release rate was calculated to be approximately 218 kW. Indicating that fires with heat release rates between 5–20kW are well within that range of fuel-controlled fire.

The small-scale room was placed under a hood for smoke gas extraction, and the temperature, pressure and oxygen concentration was measured in the duct in order to be able to calculate the energy release rate. Two thermocouple trees were installed. For measurements of the hot gas layer temperature, one of the thermocouple trees was placed in the corner opposing the burner, and another thermocouple tree was placed

in the opening of the compartment. A handheld burner was used to start the fires. The gas burner was placed to correspond with the different fire positions. The same procedure with placement was made for the liquid fuel source. To measure the plume temperature a handheld thermocouple was moved in above the fire after 15 minutes had passed for each test and measurements were taken roughly every other second. As mentioned previously, each test took one hour. 15 minutes for burning in an attempt to reach steady-state conditions, followed by between 20–45 minutes of waiting to allow the compartment to cool down in order to have similar compartment temperatures when starting each test. The temperature of the walls was measured with a handheld laser thermometer to determine when the compartment was cool enough to start the next test. The flame height was measured visually after 10 minutes and a photo and video were taken to help validate the observations.

4.2.5 Averaging gas layer temperatures

An established approach to determine the average gas layer temperatures of the upper and lower layers from experimental results was used in order to achieve accurate approximations. In this thesis the method known as Quintiere's method was used, the method, proposed by Quintiere, Steckler, and Corley in 1984 was further refined by McGrattan, Hostikka, Floyd, McDermott, and Vanella in 2021. In Quintiere's method, the upper layer temperature is determined by solving two integrals, as seen in equation 31 and 32.

$$(H - z_{\text{int}})\, T_{\text{u}} + z_{\text{int}}\, T_l = \int_0^H T(z)\text{d}z = I_1 \tag{31}$$

$$(H - z_{\text{int}})\, \frac{1}{T_{\text{u}}} + z_{\text{int}} \frac{1}{T_l} = \int_0^H \frac{1}{T(z)}\text{dz} = I_2 \tag{32}$$

with z as the height above the floor where $z = 0$ is the floor and $z = H$ is the ceiling and z_{int} is the interface height, T_u is the upper layer temperature and T_l is the lower layer temperature. These two equations are then solved for z_{int} according to equation 33.

$$z_{\text{int}} = \frac{T_l \left(I_1 I_2 - H^2\right)}{I_1 + I_2 T_l^2 - 2 T_l H} \tag{33}$$

The value of T_l can be taken as the temperature reading from the lowest placed thermocouple in the experiment as a similar procedure to the calculational procedure suggested by McGrattan et al. (2021b).

4.3 Simulations

Simulations were performed in FDS version 6.7.9 to replicate the tests with propane with the heat release rates of 5, 10 and 20 kW, to determine if the results from FDS agree with the experimental results, and/or by how much the result differs. An example of the code can be found in Appendix 2 - FDS code. No simulation of the liquid fuel was performed.

4.3.1 Procedure

The computational domain was set up using PyroSim. The small-scale ISO room was replicated as shown in figure 16.

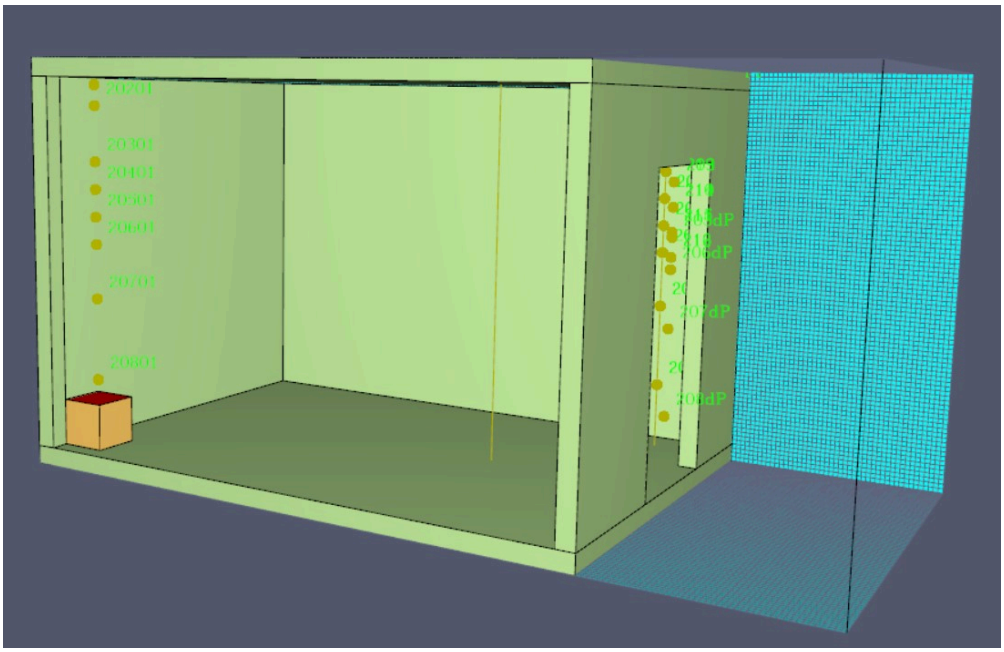

Figure 16: The layout of the room that was simulated in FDS. The fire is visible in one of the corners, and devices are shown. One wall is made invisible to get a visual view of the interior of the room.

For the material data for fibre silicate board, values for density, specific heat capacity and conductivity are taken from Dittmer and Jämtäng (2006). A number of devices were placed in the room to replicate the placement of the thermocouples and pressure meters in the experiment, the devices were given properties of thermal beads, in order to as closely as possible replicate the behaviour of thermocouples.

$D^*/\delta x$ was calculated using equation 25 to determine mesh resolution. Only one mesh was used in the computational domain, to avoid problems with fine turbulence structures causing problems when transferred between mesh sizes. Using a mesh resolution of 0.01 m for the mesh gave $D^*/\delta x = 11.5$ for the 5 kW fire, $D^*/\delta x = 15.2$ for the 10 kW fire and $D^*/\delta x = 20.0$ for the 20 kW fire, these values are within the acceptable range as mentioned in section 2.2. The 1 cm mesh was simulated for around 200 seconds, in order to perform a mesh sensitivity analysis. For computational reasons, the full-time simulations of 900 seconds were performed using a 2 cm mesh. $D^*/\delta x$ for the 2 cm mesh gave $D^*/\delta x = 5.6$ for the 5 kW fire, $D^*/\delta x = 7.6$ for the 10 kW fire, and $D^*/\delta x = 10.0$ for the 20 kW fire. The mesh was placed so that the computational domain included the solid walls, to account for heat transfer into the walls, floor and ceiling. As mentioned, a mesh sensitivity between the 1 cm and 2 cm meshes was performed by simply comparing the different hot gas layer temperatures from the simulations using the two different meshes.

$\dot{Q}^*$ was calculated using equation 26, resulting in a value of 2.1 for the 10 kW fire and 4.2 for the 20 kW fire. The value for the 20 kW fire is higher than the specified maximum value of 2.5, but as mentioned in chapter 2.2, a value greater than 2.5 is assumed to be

reasonable due to the natural momentum that occurs from the gas burner and to avoid deviating from the experimental setup.

4.4 Hand calculations

By using old experimental data from previous experiments in the same compartment, material data was collected where the effective heat transfer coefficient, h_k was the important parameter to be able to calculate the temperatures in the hot gas layer using the MQH method. h_k was calculated with experimental data and by taking an average to be approximately 0.015 kW/m^{2}K and with theoretical calculations using material data from Dittmer and Jämtäng (2006) and by approximating the values between 600 and 900 seconds the value of h_k was calculated to be 0.0152 kW/m^{2}K. The difference between these two values causes a marginal difference in temperature.

Hand calculations using different equations for different variables were used to gain an estimated result to compare with both the experiment and the simulations. Some of the equations that were used are Heskestads flame equations 1, 4 and 5 to determine the mean flame height, plume temperature and virtual origin. To start calculating flame height equation 26 was used to find the dimensionless heat release rate, $\dot{Q}^*$. As mentioned in the theory, chapter 2.1.1, the dimensionless heat release rate should be in between $0.4 < \dot{Q}^* < 2$ in order to use an unmodified flame height correlation. This is not the case for both the 10 kW and 20 kW fires, as $\dot{Q}^*$ are 2.85 and 5.69 respectively. Modification of wall and corner configuration was performed with the flame height being calculated using equation 2 and 3. In the theory, chapter 2.1.1, it is also stated that a fire with a square burner located directly against a corner or wall could have a flame height twice as high as a free-burning fire. To account for this the 5 kW fire is also modified for the wall and corner configuration even though $\dot{Q}^*$ was 1.42. Flame height in both the experiment and calculations was capped at 0.8 metres since that is the height of the compartment.

The plume temperature was calculated at a height of 0.78 m from the floor of the compartment. Plume temperature was assumed to not reach above the maximum flame temperature, Lattimer and Sorathia (2003) conducted a series of experiments and found that a maximum temperature increase for corner configurations using a propane sand burner is in the vicinity of 950 ℃. The MQH method using equation 8, 9 with the addition of 10a or 10b was used to determine hot gas layer temperature. Predictions with modification factors were made.

To determine if the plume mass flows, mass flows out of the compartment opening equation, 12, 13, 19, 20 and 21 was used. At steady state $m_g = m_p$ where the height of the neutral plane was calculated using the method from chapter 2 and the following equations, 22, 23 and 24. In the equations for m_p, a simplification was made for the height of the hot gas layer by setting the height of the hot gas layer to be the height of the neutral plane.

As mentioned previously the dimensions that were used for the room in calculations were $0.8 \times 1.2 \times 0.8$ m with a door measuring 0.27×0.67 m. The area of the gas burner was $0.1 \times 0.1 \times 0.1$ m, which gave a diameter of approximately 0.113 m. Density was determined as $350/\mathrm{T_a}$ where $\mathrm{T_a}$, the ambient temperature was taken from the laboratory at the time of the experiment, $T_a = 18$ ℃. The acceleration of gravity was assumed to

be 9.81 m/s^2. Specific heat capacity for air was taken as 1.005 J/kgK. For the small scale room A_0 was approximately 0.178 m^2, H_0 was 0.667 m, A_t was 4.94 m^2 and h_k was 0.015 kW/m^2K which has been calculated based on data from previous experiments using the small-scale test room.

5 Results

In the following section, results will be presented for each test in the laboratory, simulations and hand calculations. Experiment 1 and experiment 2 with propane had the same experimental setup. The only difference was that experiment 1 was conducted another day as experiment 2 to avoid the potential impact of ambient conditions, due to the need for an open door during the experiments for makeup air. The same applies to the experiments with liquid heptane.

5.1 Opening mass flow

Opening mass flow from the experiment was calculated using values from the pressure meters and thermocouples located in the door opening and the plume mass flow was estimated based on the fact that $m_g = m_p$. The method is presented in chapter 2. The same method is applied to the simulations to be able to compare values using the same method. In the simulations, the mass flow in and out of the compartment was also measured using a mass flow device in the opening of the compartment. The mass flow from hand calculations for both the experiment and the simulations are calculated with equations 13, 19 and 20, with the said assumption that $m_g = m_p$.

In figure 17 the mass flow using values calculated with the pressure difference and temperature readings are plotted against the theoretical values from equations 13, 19 and 20. Values from both experiment 1 and experiment 2 are presented in the figure.

Table 8: Mass flow out from the compartment for the experiment (average value) and simulations in FDS, calculated using pressure meters (PM), devices in FDS and hand calculations using Zukoski's plume flow equation.

	Experiment		Simulations		
	PM (kg/s)	Zukoski (kg/s)	PM (kg/s)	Devices (kg/s)	Zukoski (kg/s)
Corner 5 kW	0.018*	0.018	0.025	0.026	0.017
Wall 5 kW	0.018	0.025	0.027	0.031	0.021
Centre 5 kW	0.023	0.037	0.035	0.038	0.024
Corner 10 kW	0.021	0.020	0.032	0.035	0.020
Wall 10 kW	0.023	0.031	0.032	0.039	0.025
Centre 10 kW	0.025	0.047	0.039	0.046	0.029
Corner 20 kW	0.025	0.024	0.038	0.047	0.022
Wall 20 kW	0.029	0.036	0.036	0.048	0.028
Centre 20 kW	0.026	0.059	0.044	0.054	0.033

* this is an average value between values 0.023 and 0.013 kg/s from experiments 1 and 2.

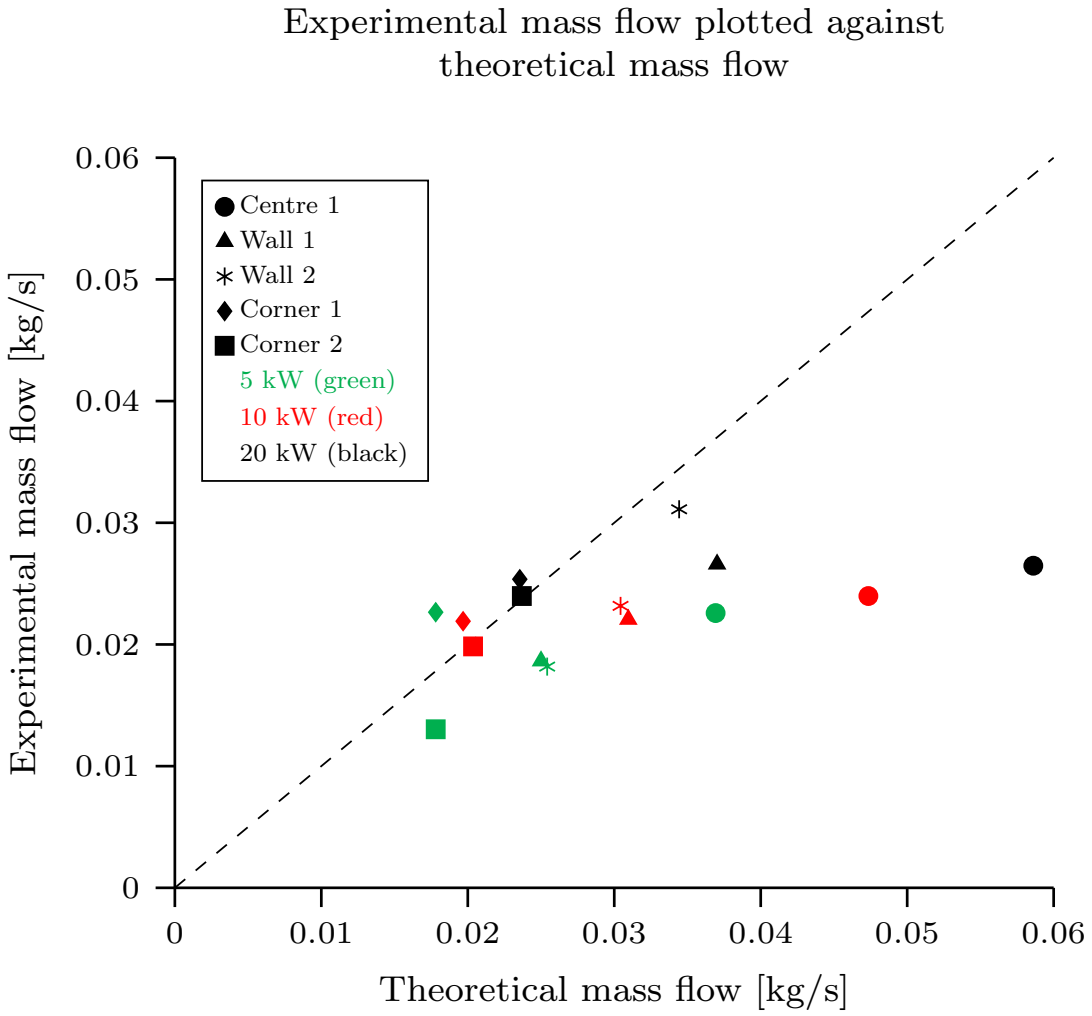

Figure 17: Calculated mass flow from the experiment using pressure meters (column 1 in table 8 compared to theoretical values using the Zukoski equations (column 2 in table 8).

5.2 Hot gas layer temperatures

To reduce the experimental temperature measurements to a value of the hot gas layer temperature, equations 31, 32 and 33 were used. As mentioned in the theory, the temperature from the lowest placed thermocouple at 0.15 m above the floor was used as the value for T_l. The results are presented in figures 18, 19, 20, 21 and summarised in table 9 with the addition of the temperatures of the hot gas layer from the simulations in FDS.

Table 9: Hot gas layer temperatures from the experiment, simulations in FDS and hand calculations using MQH correlation.

	$T_{g,exp}$ (°C)	FDS (°C)	MQH (°C)
Corner 5 kW	138	160	174
Wall 5 kW	106	126	137
Centre 5 kW	108	105	110
Corner 10 kW	209	247	265
Wall 10 kW	168	200	207
Centre 10 kW	166	168	163
Corner 20 kW	302	362	410
Wall 20 kW	264	312	318
Centre 20 kW	252	272	249

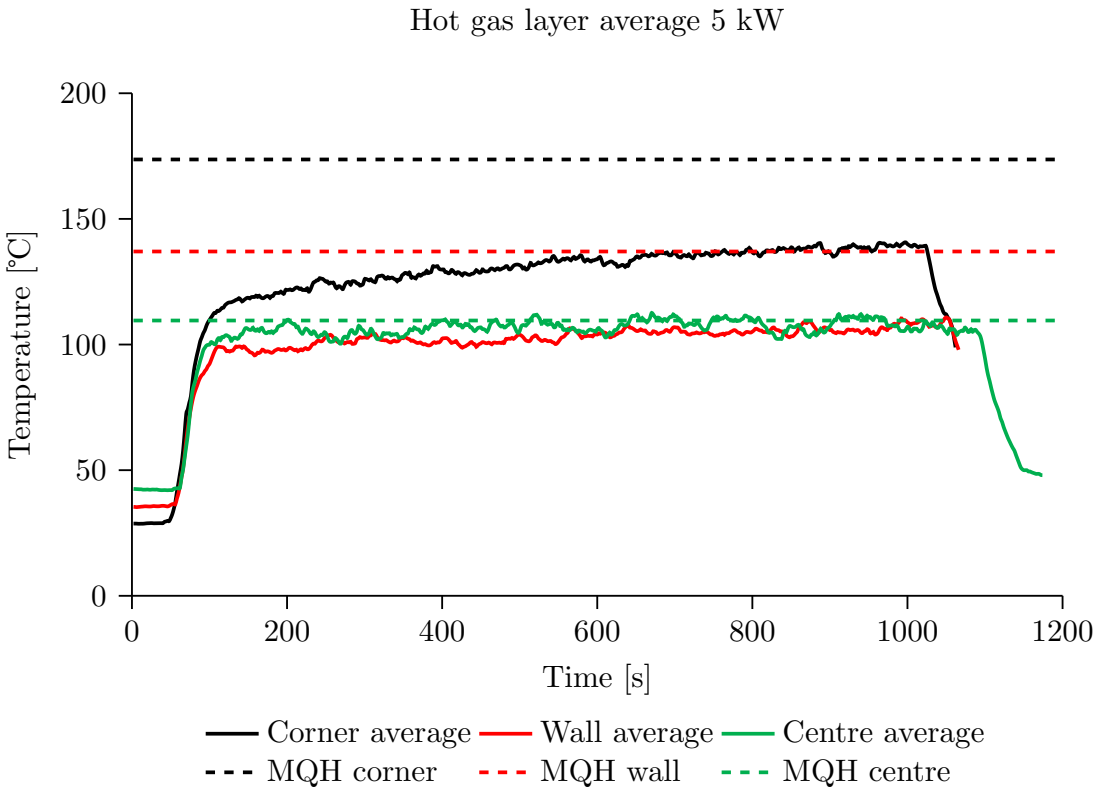

Figure 18: Average hot gas layer temperature for corner, wall and centre fires with gaseous propane and 5 kW. The dashed line is the result of the MQH correlation for each position.

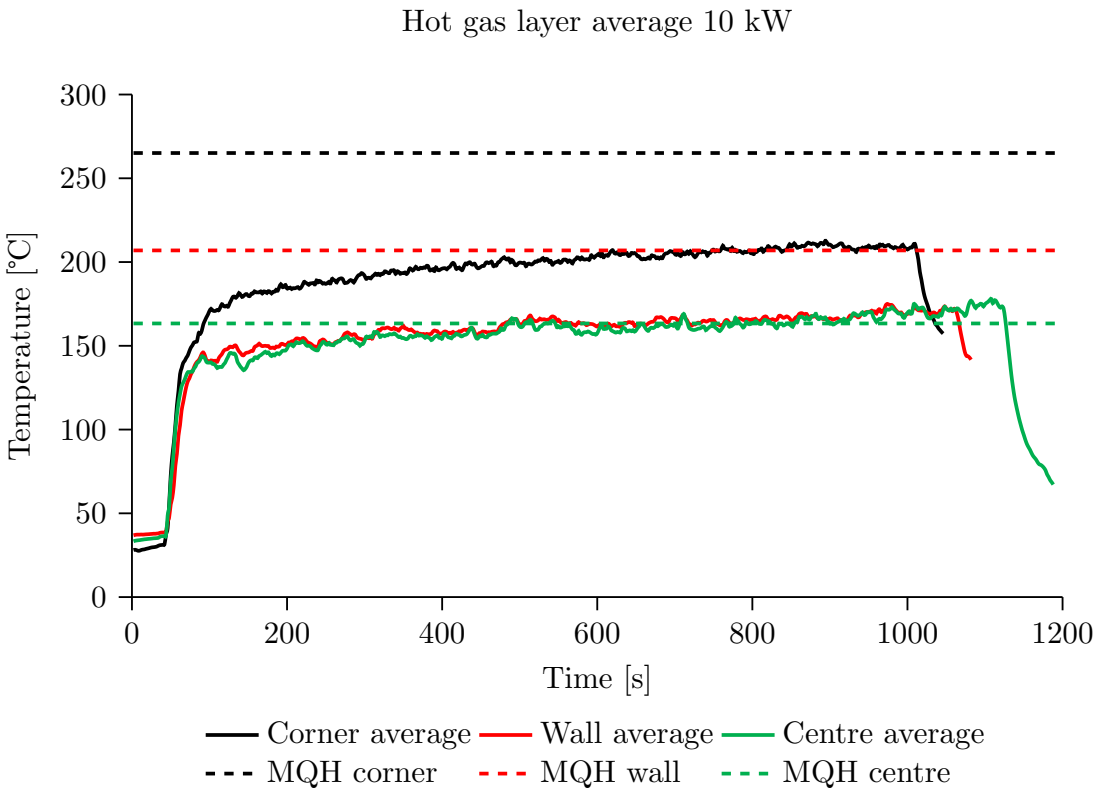

Figure 19: Average hot gas layer temperature for corner, wall and centre fires with gaseous propane and 10 kW. The dashed line is the result of the MQH correlation for each position.

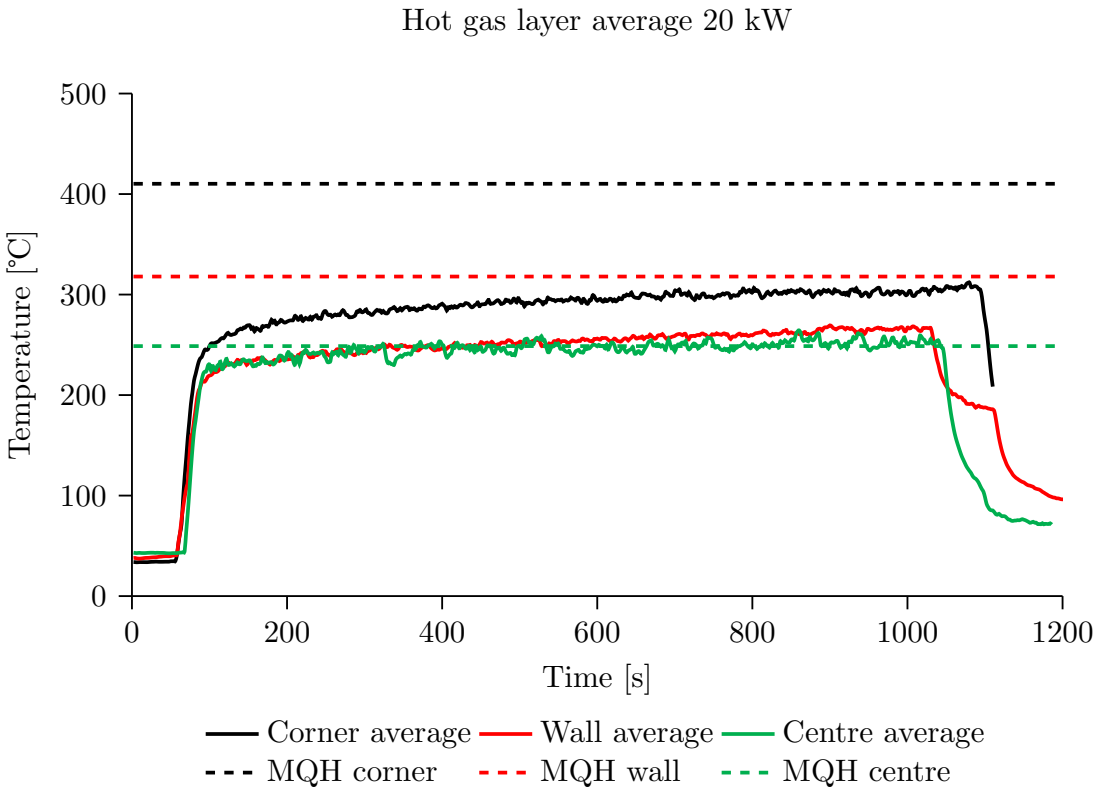

Figure 20: Average hot gas layer temperature for corner, wall and centre fires with gaseous propane and 20 kW. The dashed line is the result of the MQH correlation for each position.

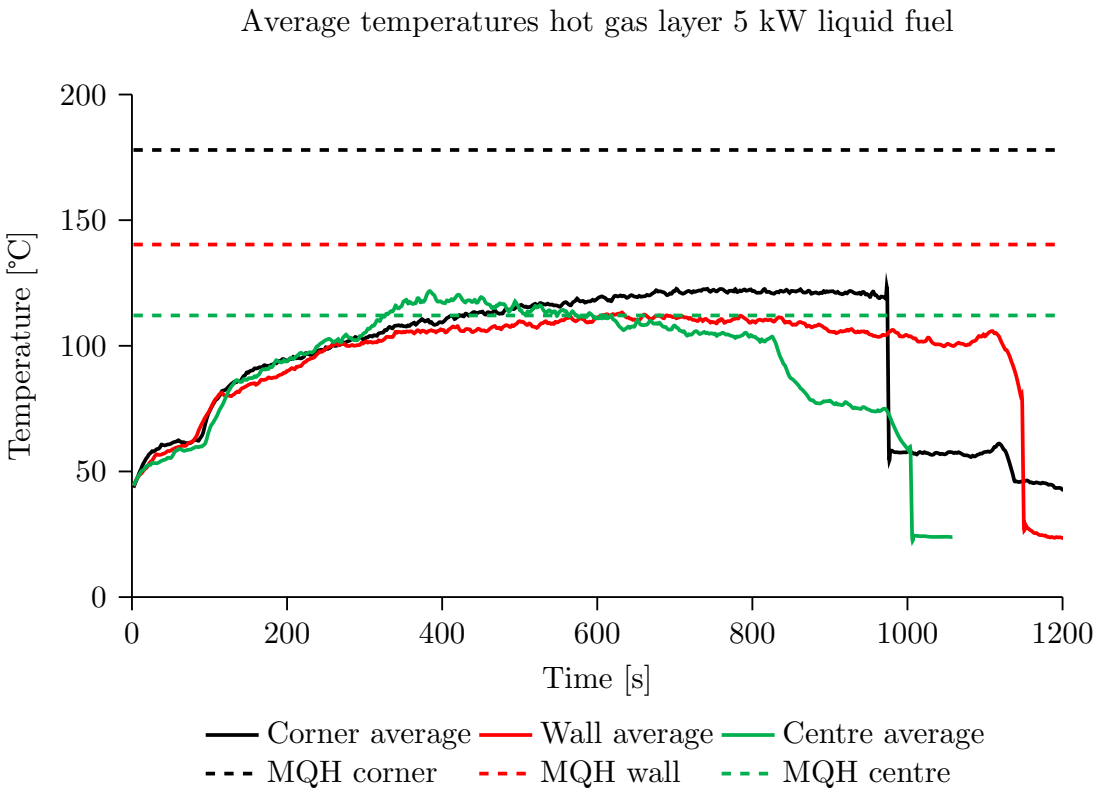

Figure 21: Average hot gas layer temperature for corner, wall and centre fires for 5 kW with liquid heptane. The dashed line is the result of the MQH correlation for each position.

The average hot gas layer temperatures from the experiment and the theoretical temperatures using the MQH correlation were compared to each other in a diagram, see figure 22.

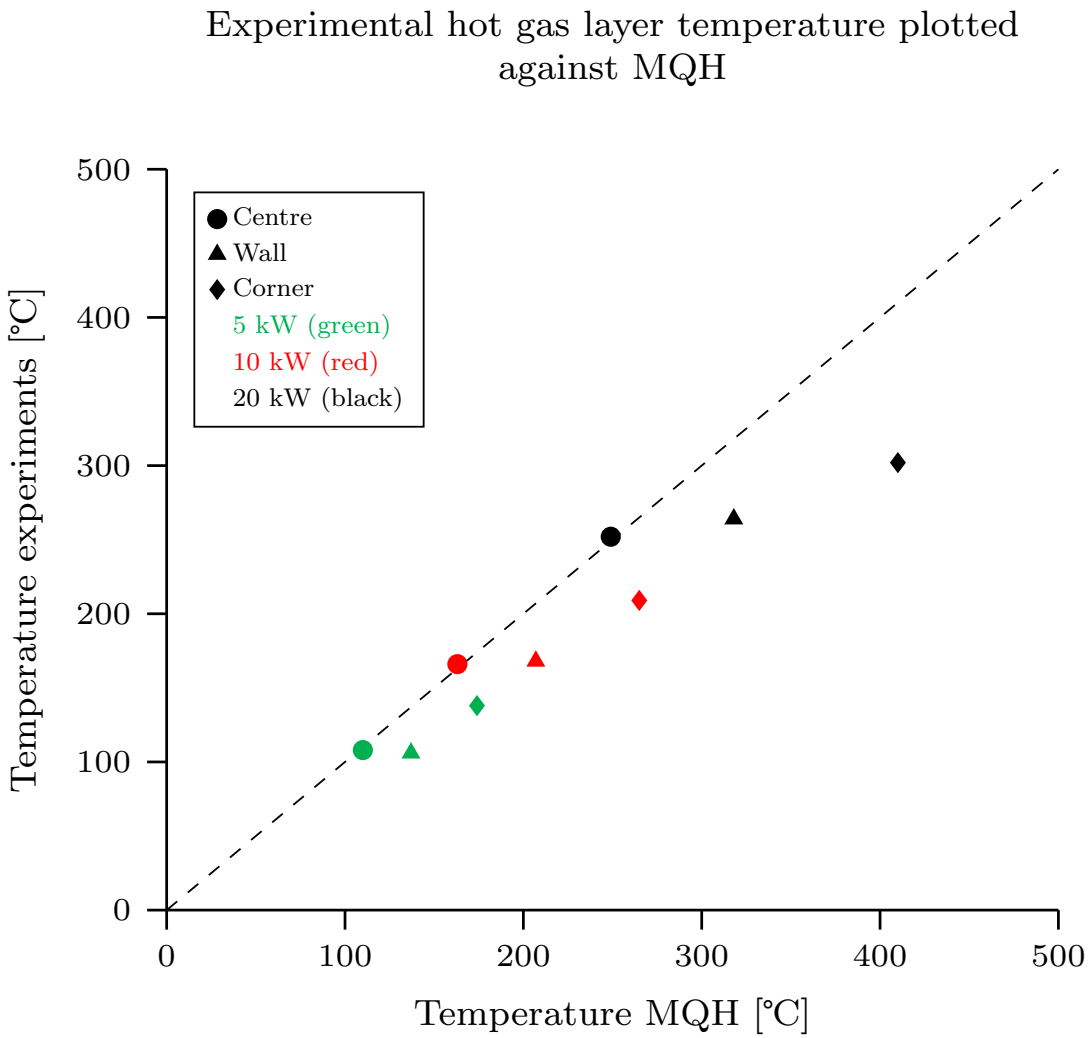

Figure 22: Measured temperature of the hot gas layer compared to theoretical temperatures using the MQH correlation and modified MQH.

The average hot gas layer temperatures from the simulations in FDS and the theoretical temperatures using the MQH correlation were compared to each other in a diagram, see figure 23.

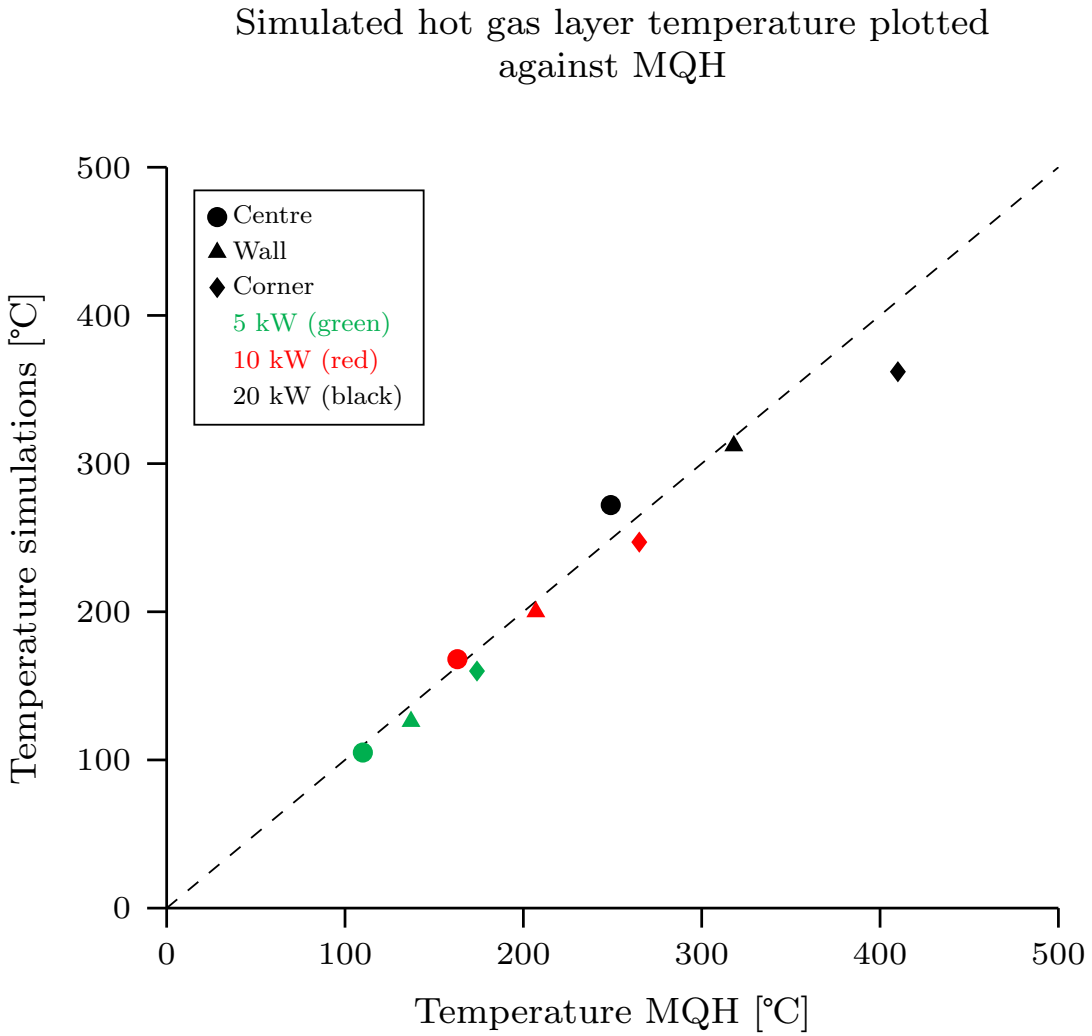

Figure 23: Temperature of the hot gas layer from simulations in FDS compared to theoretical temperatures using the MQH correlation.

The average hot gas layer temperatures from the experiment and average hot gas layer temperatures from the simulations in FDS were compared to each other in a diagram, see figure 24.

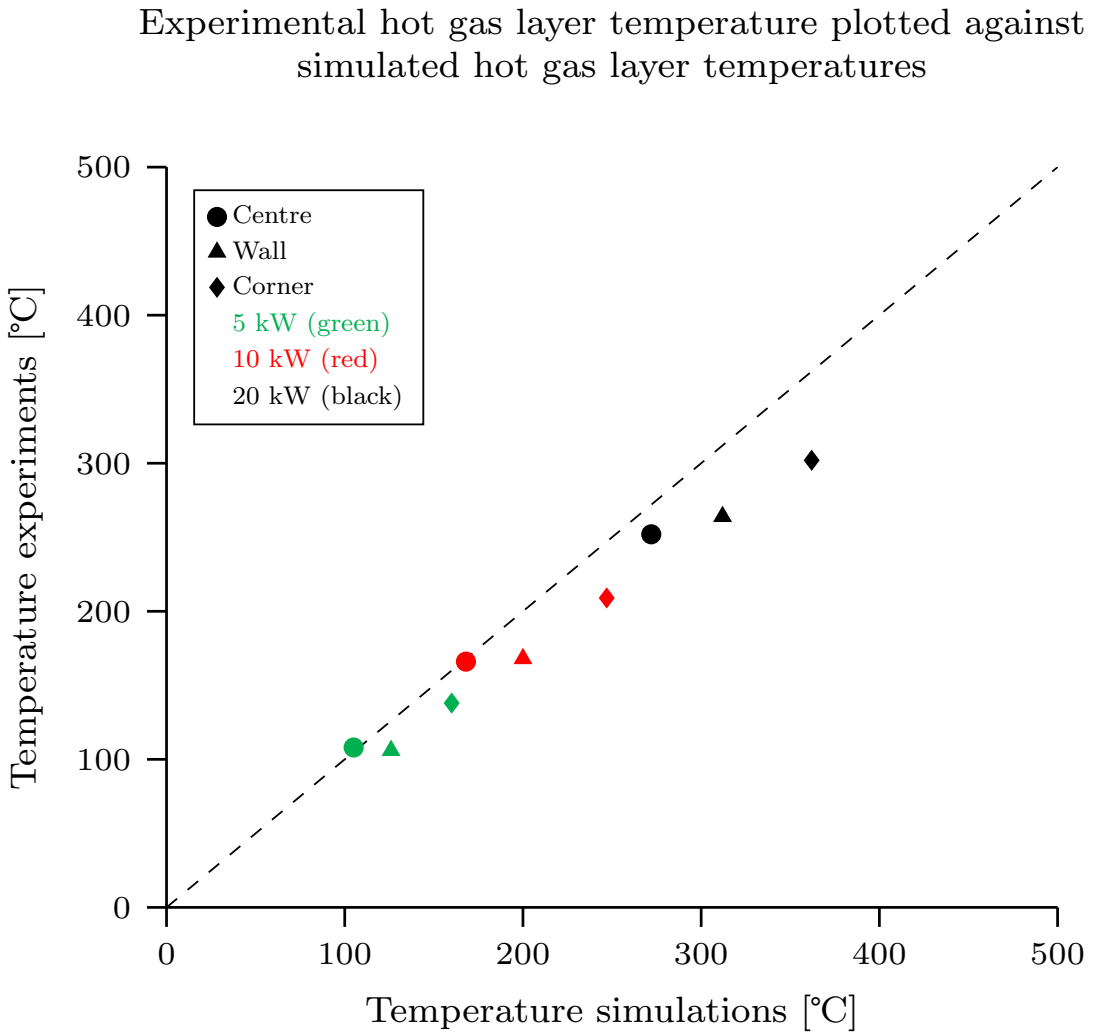

Figure 24: Measured temperature of the hot gas layer compared temperatures of the hot gas layer from simulations in FDS.

5.3 Flame heights

The following figures, figure 25, 26 and 27 show the flame height at each corresponding heat release rate. The height was visually observed and photographed at about 10–15 minutes after each test started.

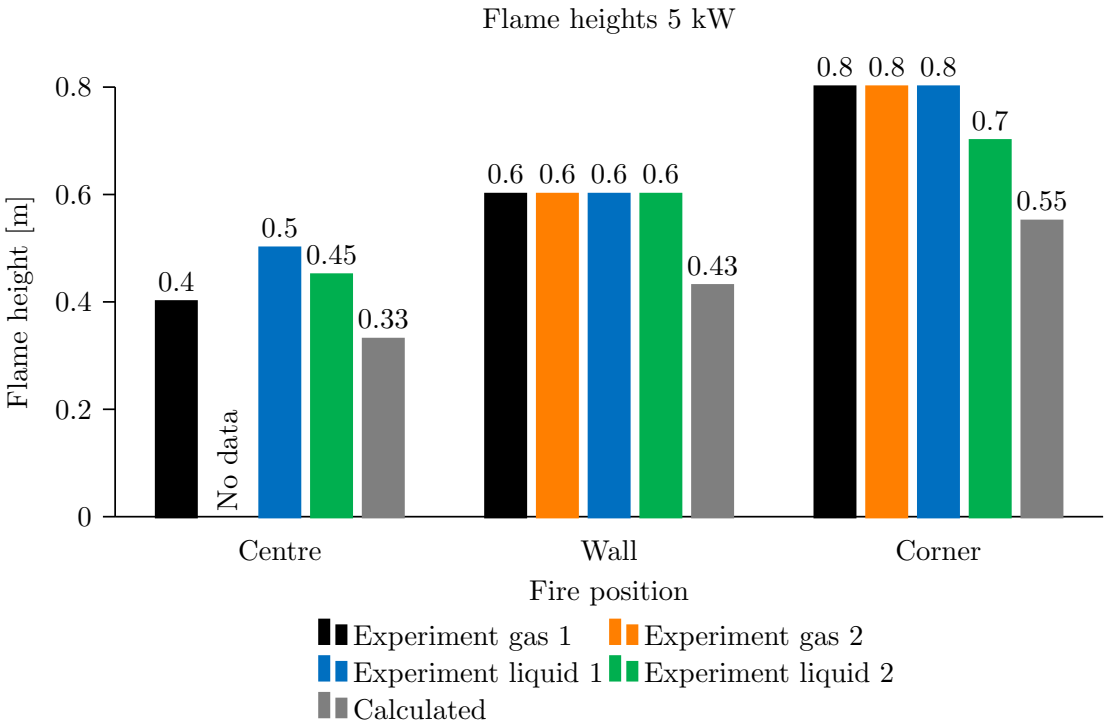

Figure 25: Measured and calculated flame heights using observed heights and recordings at 5 kW.

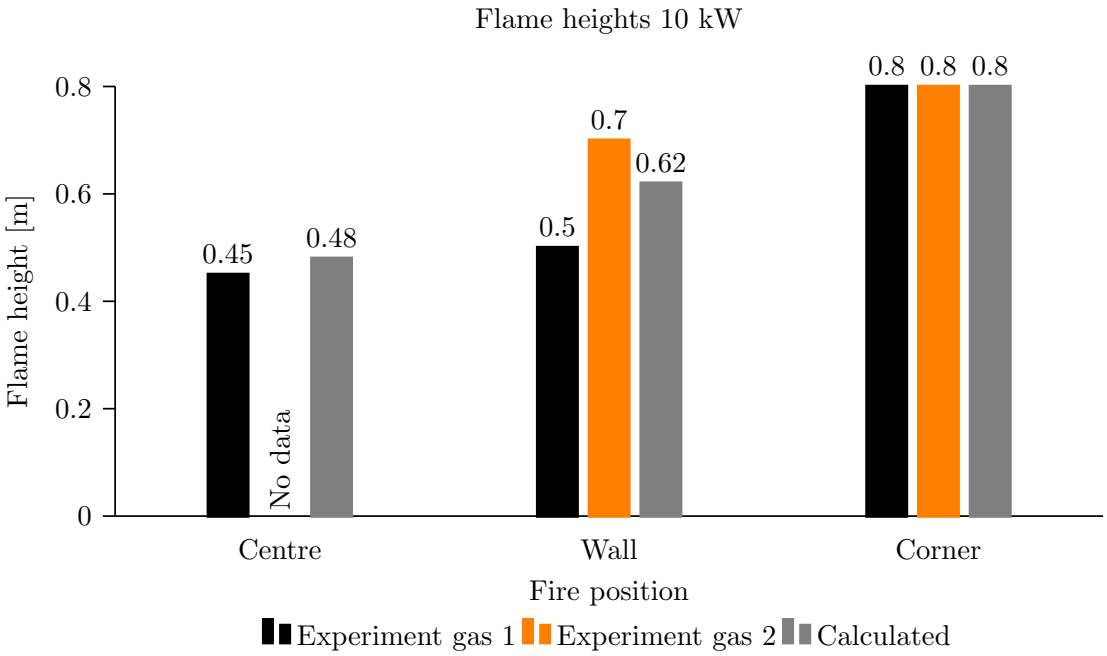

Figure 26: Measured and calculated flame heights using observed heights and recordings at 10 kW.

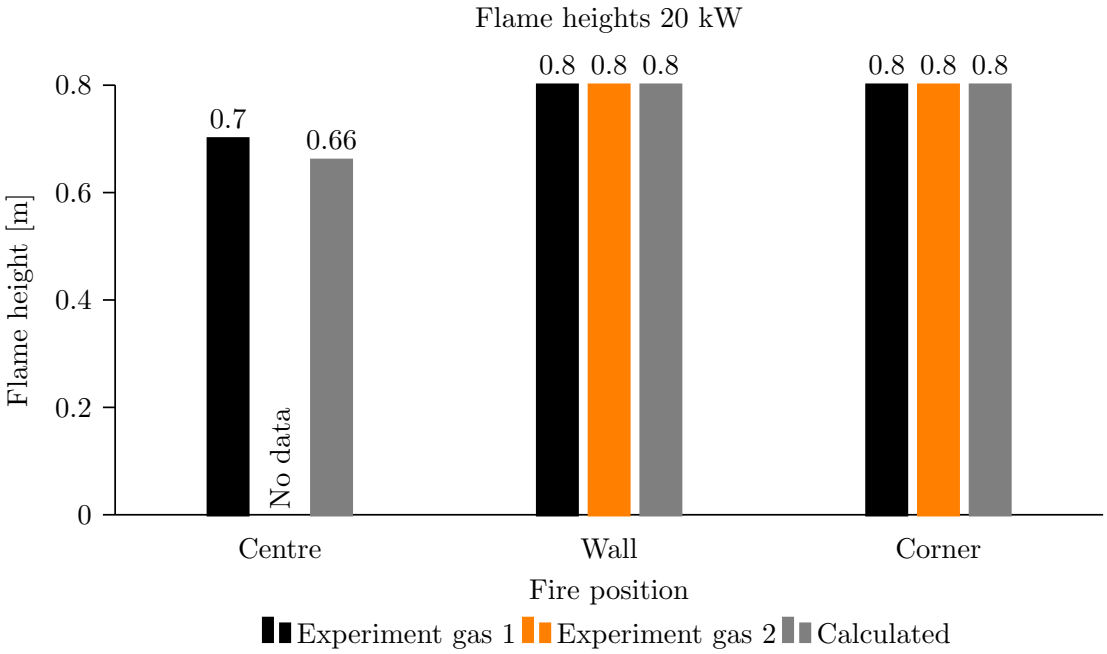

Figure 27: Measured and calculated flame heights using observed heights and recordings at 20 kW.

5.4 Plume temperatures

The plume temperature, which was measured with a handheld thermocouple approximately 0.02 m below the ceiling, is presented in figures 28, 29 and 30, together with the theoretically calculated value using the Heskestad correlation. Note that the measurements are taken in the hot gas layer, which might cause problems when compared with the theoretical value. The measurements were taken after 15 minutes as described in chapter 4.2.4.

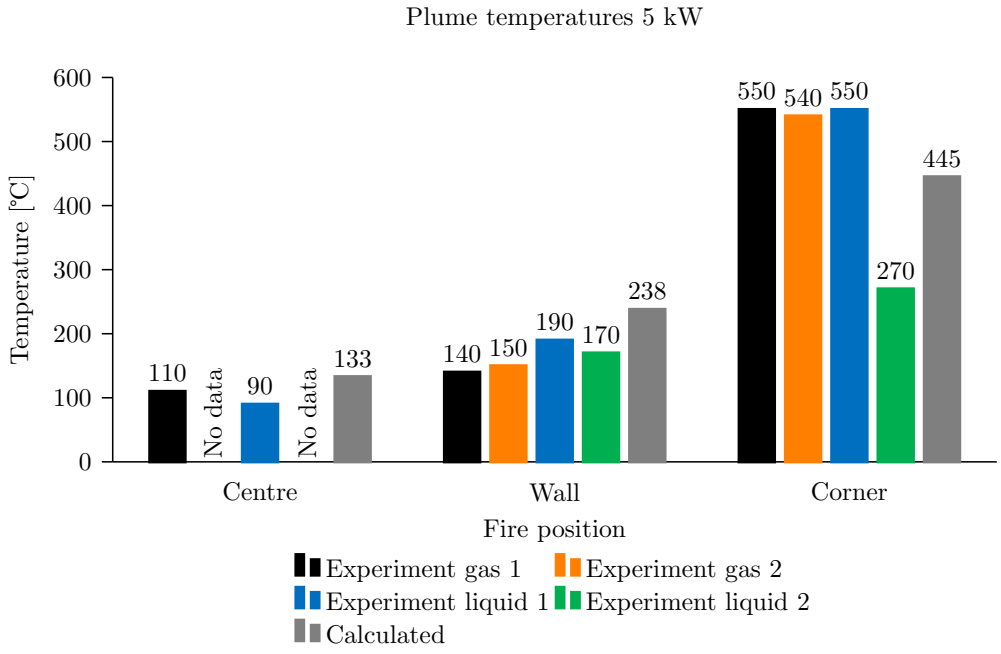

Figure 28: Measured and calculated plume temperatures at 5 kW.

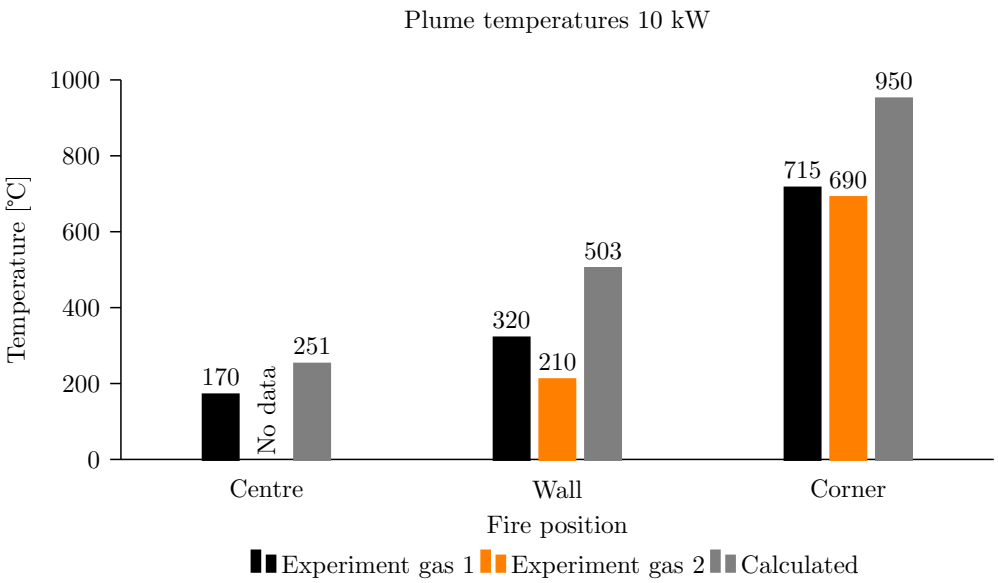

Figure 29: Measured and calculated plume temperatures at 10 kW. Note that the calculated value for the corner is calculated outside the valid range of the Heskestad correlation

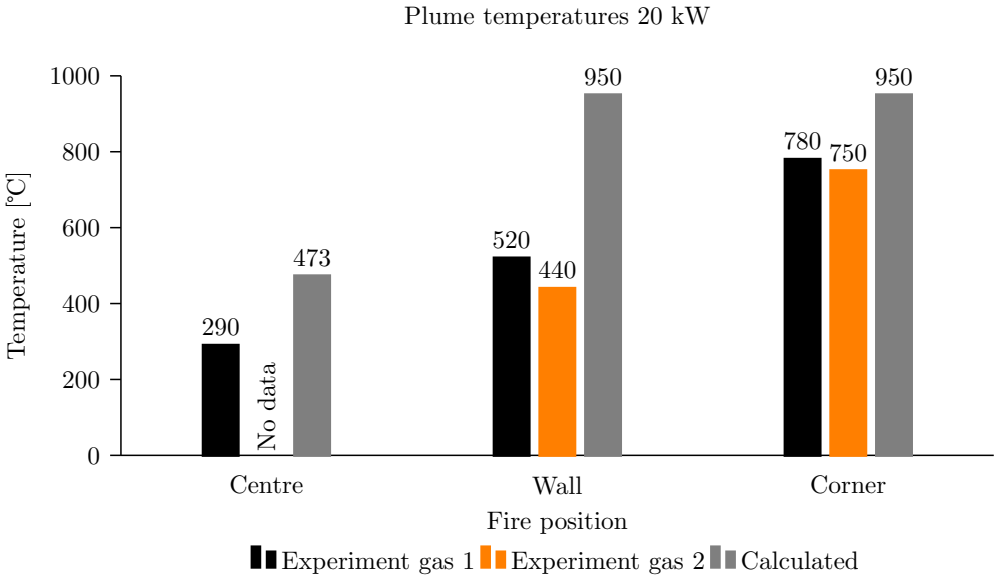

Figure 30: Measured and calculated plume temperatures at 20 kW. Note that the calculated value for corner and wall is calculated outside the valid range of the Heskestad correlation

6 Discussion

In the following section, the result from the experiment, simulations and hand calculations will be discussed and compared with previous studies and experiments conducted by amongst others Mowrer and Williamson (1987) and NIST's study performed by McGrattan, Selepak, and Hnetkovsky (2018). Hence in the following discussion, problem statements 1-5 will be addressed in the following sections, 6.1.2, 6.1.3, 6.1.4 and 6.2.

6.1 Experiment

6.1.1 Plume mass flow

The approximations for mass flow using results from the pressure meters give mass flows for the centre fire that are unrealistic in regards that the mass flow only increased slightly between the heat release rates. The difference in heat release should be more according to theoretical calculations using the Zukoski plume mass flow equation. The difference in increase between the mass flow rates differs by almost one order of magnitude. The mass flow rates from the experiment are also continuously underestimated when compared to the results using the Zukoski plume mass flow equation. However, it should be noted that when studying the results from the simulations, comparing the two methods for calculating mass flow, the pressure meter method and the mass flow devices, the pressure meter method gives lower mass flux than the mass flow devices. This indicates that the pressure meter method might continuously underestimate values of the mass flow from the compartment. The values from simulations when using Zukoski's plume mass flow equation might also have some errors in it. To determine if Zukoski's plume mass flow equation was problematic, another plume equation proposed by Heskestad, Equation 14 and 15 was utilised and compared to the experimental results. In this comparison, it was clear that Zukoski's plume mass flow was closer to the experimental results eight out of nine times. Both plume equations followed the same trend of higher plume mass flow in the centre configuration and lower plume mass flow for the wall configuration and even lower for the corner configuration. However, it is worth noting that Heskestad's plume equations were closer to the simulated mass flow using FDS eight out of nine times. As mentioned in the theory chapter 2, the Zukoski plume is valid when the flame height is lower than the height of the hot gas layer which was not achieved during several experiments, especially for the ones in the corner configuration. The difference in results could be attributed to the different profiles used in each equation. Heskestad should fit better for the corner configuration due to the equation being valid when the flame is in the hot gas layer.

The height for the hot gas layer calculated by FDS does not correspond entirely with the observed values from the experiment. For example, the value that FDS gives for hot gas layer height for 5 kW, centre position, was 0.36 metres, compared to an approximate value of around 0.6 metres in the experiment. No further analysis will be made on this question.

6.1.2 Hot gas layer temperatures

The hot gas layer temperature is shown in figure 18, 19 and 20. It is clear from these results that the hot gas layer temperature is higher when the fire is placed in a corner compared to a centre or wall placement. The relationship between corner, centre and wall placements does not change with an increased heat release rate. McGrattan et al. (2018), Mowrer and Williamson (1987) and Yunlong and Vivek (2004) also present results with an increase in temperatures regarding fire placement when comparing the corner configuration and centre configuration. The difference in this thesis compared to Yunlong and Vivek is that the temperatures in these two configurations are not as big but there is still a 50–100 ℃ difference when comparing with the same HRR based on compartment size.

The measured temperatures of the hot gas layer and the theoretical value from the MQH correlation are plotted against each other in figure 22. It is clear that the unmodified correlation for the centre fire agrees well with the measured temperatures from the experiment. For the fire against the wall and in the corner, the MQH correlation overestimates the temperatures in the hot gas layer. The major thing to note about the comparison is that the temperatures from the experiment for the wall fire are almost the same as temperatures for the centre fire, which is a very important difference between the experiment and the MQH correlation. The lines might seem to follow some trend, but it is determined that there are not enough data points to determine if the slope of the lines is linear or logarithmic for the wall and corner fires.

A conclusion about the correlation of the temperatures can be drawn from figure 23. The centre fire results from the simulations seem to correspond rather well with the unmodified MQH correlation. However, the results from the wall simulations and especially the corner simulations seem to differ from the results from the MQH correlation with the modification factors. The most important difference from figure 22 is that the simulations did give an increased temperature for the wall fires compared to the centre fire, whereas the experiment did not. The three lines are closer together which shows an increased correlation between the results from the simulations and the MQH correlation. An interesting thing to note is the similar appearance between figures 22 and 23. When studying figure 24, it is easy to be deceived into thinking that the experimental results and the simulation results seem to correlate fairly well with each other, but again, the major difference between the experimental results and the simulations are the increase of the temperatures from the wall fires compared to the centre fires which occurs in the simulations, but not in the experimental results.

Compared with the results from Mowrer and Williamson (1987) there are a couple of differences from the results in this thesis. First, there is no discernible difference between the temperatures in the hot gas layer when comparing the centre configuration and wall configuration, compared to the result of Mowrer and Williamson, which did gain a difference in hot gas layer temperatures. The second big difference is that the modification factors to the MQH method proposed by Mowrer and Williamson, do not fit the results from this thesis. As seen in figure 18, 19 and 20, the MQH method almost perfectly aligns in the centre configuration where no modification factor was used. However, both wall and corner configurations are shy of the calculated value with approximately 100 ℃. While the parameters that determine h_k might change the relationship between the centre and corner configuration values that are calculated, it will also cause the approximation of the centre configuration to stray away from the

well-matching value between the experiment and the MQH correlation. The results in figure 19 where the heat release rate is 10 kW, compare to an up-scaled heat release rate of 160 kW in the full-scale experiments performed by Mowrer and Williamson. This means that the temperatures should be somewhat similar if the compartment properties were the same. Some other deviations are from the experimental setup, where Mowrer used a gradual increase in heat release rate from 40 kW to 80 kW to 160 kW with 5 minutes at each heat release rate, while in this thesis the tests started at maximum heat release rate in all of the tests and held it at that level for the complete 15 minutes. However, both methods should have reached a steady state. The result in this thesis is temperatures in the hot gas layer that is approximately 150 ℃ lower compared to the results from Mowrer and Williamson. As mentioned in chapter 3 the experiment performed by Mower had a compartment lined with gypsum wallboard, which, if using data from Karlsson and Quintiere (2022), has the properties $\rho = 668$–1000 kg/m^3, $c_p = 0.95$ kJ/kgK, conductivity k = 0.254–0.314 W/mK and emissivity $\epsilon = 0.8$–0.9. This is different from this thesis, as the compartment for the experiment had walls made out of fibre silicate board, with properties $\rho = 870$ kg/m^3, $c_p = 1.13$ kJ/kgK, conductivity k = 0.175 W/mK and $\epsilon = 0.9$. When comparing the two materials parameters it is noticed that with a lower conductivity and a higher specific heat the fibre silicate board used for the experiment in this thesis should cause higher temperatures than the gypsum boards, however, that is not the result of the experiment. This could have been caused by cracks in the compartment and the fact that this compartment has been used several times before this experiment which might have deteriorated the materials original properties.

The results from this thesis when comparing the hot gas layer temperature relationship between a centre and wall configuration is more aligned with the results from McGrattan et al. (2018). However, it is important to note that the temperatures from the experiments conducted by McGrattan et al. came from measurements on plume temperature and calculations with the Heskestads correlation and not the hot gas layer temperature using MQH. McGrattan et al. did measurements on the hot gas layer temperature but did not find any significant change in the temperature between the different positions. One speculation from the authors of this thesis is that the large compartment used by McGrattan et al. combined with the placement of the thermocouples used to measure the hot gas layer temperature gave those results.

Similar to the results with propane, the calculated values for the hot gas layer using the MQH correlation do not match the measured experimental values for liquid fuel, as seen in figure 21. As mentioned in section 2, pool fires are affected by radiative heat flux from the flame and other surfaces toward the fuel surface (Karlsson & Quintiere, 2022). This might have caused the deviation from the calculated heat release rate of the fire for the centre configuration. Both the wall and corner stayed at around the calculated value of 5 kW with a maximum of 5.6 kW. This is also reflected in the results, where the corner configuration resulted in higher temperatures than the wall configuration, with temperatures similar to tests with propane with the same heat release rates. The centre configuration starts by gaining higher temperatures in the hot gas layer than both the corner and wall configurations. A possible explanation for this is that the view factor for the radiative heat flux from the hot gas layer towards the fuel surface is higher than in the wall and corner configurations. There was a deviation from the calculated heat release rate of 5 kW to the actual heat release rate with a maximum value of 8.3 kW. Due to this, the hot gas layer temperature is only compared for the

wall and corner position with the results using gaseous propane in figure 18. The hot gas layer temperature produced by gaseous propane reached a maximum temperature of 150 ℃ for the corner configurations, while the liquid heptane produced a hot gas layer temperature of 123 ℃. For the wall configuration, heptane produced a hot gas layer with a maximum temperature of 113 ℃ compared to propane which produced a hot gas layer with a maximum temperature of 108 ℃. The difference is not large, with a maximum of 12 %.

When comparing the results of the tests using gaseous propane with a heat release rate of 20 kW, see figure 20, with the results from Yunlong and Vivek (2004), see figure 8, 9 and 10, the 20 kW compares to 300 kW in full scale. One difference that can be mentioned is that different gases are used. In that report, methane gas was used and in this thesis, propane is used. In figure 8 the maximum temperature is approximately 480 ℃ and the highest temperature from the experiment in this thesis is approximately 312 ℃, see figure 20. However, the measurements in 8 from Yunlong and Vivek were taken at the ceiling level in the centre of the room and the measurements in the experiment from this thesis are taken in the corner furthest away from the fire. The values from the figure 9 might be more appropriate to compare with since they are taken at the same distance from the fire as the measurements in this thesis but at a lower height. At the doorway in the experiment by Yunlong and Vivek, the maximum temperature reaches approximately 400 ℃ which still is a difference of approximately 90 ℃ from the results in the experiment in this thesis. One cause for the difference might be from the materials used on the walls in the experiment by Yunlong and Vivek, which used plasterboard wall linings, while in this thesis fibre silicate boards that had been through several experiments before was used.

One parameter that likely influences the results of the experiment is radiative heat flux from the flames towards the thermocouples. The thermocouples do not in actuality measure the hot gas layer temperature but the temperature in the thermocouple themselves. This means that depending on the distance from the fire the thermocouple will be more or less influenced by the radiative heat flux. For all tests, the centre configuration is located closest to the thermocouples followed by the wall configuration and lastly the corner configuration. The temperature measurements of the centre configuration should according to this be slightly higher than the actual hot gas layer temperature, which might have been the reason why there was no noticeable change in temperature between the centre and wall configuration. The actual hot gas layer temperature is unknown, but it is not impossible that the hot gas layer temperature for the centre configuration was lower than for the wall configuration. In hindsight, a way to reduce or measure radiative heat flux should have been implemented in the tests to be able to reduce or account for the heat flux.

From the result of this thesis, it would be more appropriate that no modification factor for the MQH correlation is used for wall configuration and that 1.3 is used as a modification factor for the corner configuration, but given the limitations, uncertainties and possible errors in this thesis, it is suggested that more experiments are conducted regarding the subject.

6.1.3 Flame height

The fuel source impact on the flame height is shown in figure 25, in which it can be observed that liquid heptane produces results that are fairly close to the results from the gaseous propane, see figure 31 and 32 and semi-close to the calculated values. As mentioned in the theory chapter, chapter 2, visual observations of flame height tend to be slightly higher than intermittency observations using cameras and tools. This means that if the actual flame height values are about 10 % lower then these measurements are even closer to the calculated values. Overall there is not a large difference between either gaseous propane or liquid heptane, however, both of these are about the same in relation to the calculated flame height except for the flame height in the corner for liquid heptane which is a lot closer to the calculated value. In all tests, the fuel container or gas burner is placed on a platform to get closer to the corner and wall, as seen in figure 31. In figure 32 the metal cube that stabilises the gas burner is much smaller and is practically impossible to see.

Figure 31: Flame height from fire in the corner with liquid heptane at 5 kW.

Figure 32: Flame height from fire in the corner with gaseous propane at 5 kW.

In both figure 25 and 26, a similar trend of higher flame height with a fire flush to a wall in relation to the centre fire is observed. This trend is even stronger for the corner fire in relation to the fire in the centre. This trend follows the theory in chapter 2, which states that flames in corners and along walls extend upwards due to limited air entrainment into the flame.

Figure 27 shows that the measured and the calculated values are very close to each other, however for both the measured and the calculated values the flame height is capped by the height of the compartment. Flames along the walls and in the corner extend below the ceiling, which means that the equation for flame height will not be as valid for the higher heat release rates, as the flames hit the ceiling, see figure 33.

Figure 33: Flame height from gas experiment 1 sticking to corner and extending below the ceiling at 20 kW after 10 minutes.

To calculate the flame height, equation 1, 2 and 3 was used with a modified heat release rate and base diameter with a factor of 2 times for walls and 4 times for corners. These modifications are made from the argument that a fire along a wall would get a double imaginary area and a corner would get a four times larger area which in turn would give an increased heat release rate, as seen in figure 2. The flame height can also be affected by the inflow of air into the test compartment, for the corner fires the airflow will keep the fire in the corner, however for the walls, the air can cause the flames to not stick to the walls which would lower the flame height as the flames would behave more like a centre placed fire, as seen in figure 34. As seen in the previously mentioned picture the flame extends backwards due to the inflow of air into the room, which made the approximation of flame height difficult. The results of the calculations using the unmodified flame height correlation severely underestimate the flame height for 5 kW, despite $\dot{Q}^*$ being in the valid range. Instead, an approach using the modified flame height correlation, equations 2 and 3 gives more corresponding results with the experiments. The flame height is still underestimated with hand calculations despite using the modified flame height correlation, but it gives a better estimation than the unmodified correlation.

Figure 34: Flames not sticking to the wall at 10 kW after 10 minutes, potentially due to airflow.

6.1.4 Plume temperatures

Plume temperatures are presented in figure 28, 29 and 30. All three of these figures show a similar trend in plume temperatures just as flame height did. Higher plume temperatures for fires along walls compared to the centre fires and even higher plume temperatures for corner fires. The tests using gas are very consistent in the results and these have a small difference from each other. The calculated values for plume temperature in the corner for both 10 kW and 20 kW are capped at 950 ℃, however, the calculated values did extend quite further than that, but as mentioned in the method chapter the maximum temperature increase for corner configuration using propane sand burner was in the vicinity of 950 ℃. For the corner configuration with heat release rates 10 and 20 kW, as well as the wall configuration with 20 kW, the value of L is higher than z, which renders the Heskestad correlation invalid, and the correlation can therefore not be used. Similarly to the hot gas layer, the thermocouples would have shown an increased temperature when closer to the fire due to the radiative heat flux. The measurements for 10 kW and 20 kW are both taken very close to the thermocouples meaning this could also be one of the reasons why the temperatures are similar.

In figure 28 several interesting points can be observed, the calculations for the corner configuration are lower than the actual experimental results and this might be caused

by faulty measurement that might have measured the flame temperature instead of the plume temperature since the flame from the fires in the corners all reached the ceiling. Measurements might at times have been taken off the produced ceiling jets and hot gas layer temperatures. The plume might also have a higher temperature due to the fact that the equation is made for free-burning fires meaning the addition of the hot gas layer that entrains into the plume increases the temperature. It is possible to observe a large difference between the two tests with liquid heptane in the corner, and this might have been caused by bad planning. Experiment 1 for liquid heptane in the corner was the first test that was conducted and it was discovered in the following tests that the way the plume temperature was measured in that test was not accurate, as it was measured at an incorrect height. In all of the other tests, the temperature was measured at the same height. This is further enhanced by the fact that the difference between the liquid heptane tests in wall configuration barely differs and both measurements were taken at the same height.

In figure 29 and 30 an observation can be made that the maximum difference in plume temperature between these two in the corner configuration is only about 65 ℃ even though the heat release rate is double in figure 30 and that neither of these reaches the maximum temperature of 950 ℃. The reason why the difference in temperature between the two heat release rates is not higher can be due to the fact that the measurements and the calculations have been made in the flame, rather than the plume. Why neither of the tests reaches the maximum temperature is most likely caused by the Heskestad correlation not being valid for the tests as mentioned above.

In table 2 and 3 results from McGrattan et al. (2018) are presented and with these the observation that for the corner configuration the maximum difference between calculated values using Heskestads plume temperature correlation, equation 4, is about 20 % and for the wall configuration 82 % at 300 kW. For the experiment conducted in this thesis, the highest difference between the calculated values and the corner configuration is 40 % and for the wall configuration, the largest difference is 59 %. The plume temperature difference in this thesis is then for the corner configuration double that of the one achieved in McGrattan et al. and the wall is for this thesis about 25 % lower than McGrattan et al. Reasons for why the difference between this thesis results and the results from McGrattan et al. might be caused by the larger compartment size in relation to the heat release rate utilised in McGrattan et al. Another difference is also that McGrattan et al. used fixed measuring points at different heights while this thesis involved changing the position of the measuring tool manually in place to measure at the designated height while the fire was active. Another difference that cannot be shown is the influence of the ambient conditions due to the open door, ambient temperature is lowered in the laboratory due to the influx of colder air from outside and the speed at which the air flows also impacts the fire which in turn affects the plume temperature.

6.2 Simulations

For technical reasons, three different versions of FDS were used before coming to a closure with the results. Version 6.7.4 was used by mistake due to a misunderstanding, but the results from this version are never used in the thesis, more for the sake of this discussion. Version 6.7.7 was used to run the 1 cm mesh used for the mesh sensitivity analysis (Appendix 1 - Mesh sensitivity analysis), and 6.7.9 was used to run the 2 cm mesh, which the simulation result in this thesis are based upon. What was noticed when comparing the result from the different versions, was that the device measuring upper layer temperature (UPPER_LAYER_TEMPERATURE), did for some of the simulations give incorrect values of the hot gas layer temperatures. The average hot gas layer temperatures did for some of the simulations exceed the maximum temperature reading from the devices measuring temperature. This occurred in 2 cm mesh simulations running versions 6.7.4 and 6.7.7. The 2 cm simulation on version 6.7.9 gave what appeared to be correct temperatures. Strangely, as the 2 cm mesh in version 6.7.7 gave incorrect values, the 1 cm simulation in version 6.7.7 gave reasonable hot gas layer temperatures when compared to the temperature devices. As the 1 cm gave seemingly correct values, whereas the 2 cm mesh did not, it is very unlikely that it is version 6.7.7 itself that has some error, but rather the mesh size. No further analysis will be made of the behaviour between the versions and mesh sizes. Given the described problems with the hot gas layer device, and to achieve better comparison for results from simulations and results from the experiment, the integration method described in chapter 4.2.5 was used, which is the method used for calculating hot gas layer temperatures from the experiment.

The value of $\dot{Q}^*$ was above the recommended maximum value of 2.5 mentioned in section 2.2. It is however reasonable to use values over 2.5 when simulating burners that have some kind of momentum, which a propane gas burner does have. Values of $\dot{Q}^*$ of up to 10.9 has been used and validated in previous simulations (McGrattan et al., 2021a). The result from the simulations does correspond well with experimental values for the centre position, which proves that a $\dot{Q}^*$ of up to 4.2 works well within the simulations.

When studying the mesh size sensitivity analysis (Appendix 1 - Mesh sensitivity analysis), an opposite behaviour to what would be predicted can be found for the corner fire. As the higher heat release rates fires had a higher, and therefore better, value of D^*, it could be assumed that the sensitivity for the mesh size would decrease with increasing heat release rate. Instead, the opposite behaviour is found in the case of the corner fire, with increasing differences between the temperatures with higher heat release rates. One likely explanation for this is the fine turbulence structures not resolving as well in the 2 cm mesh as in the 1 cm mesh resolution, and this apparently affects the corner fire more than the wall fire and free-burning fire. As the increased flows in the higher heat release rates result in more turbulence, it is reasonable to say that a higher heat release rate would be affected more if the turbulence is not resolved in a high enough resolution.

6.3 Compartment specific error sources

As mentioned previously, the compartment used for the experiment had several cracks that might have had an impact on the result by lowering the plume temperatures, hot gas layer temperature and possibly even the flame heights. The cracks are shown in figure 35 to 39. These cracks could be one of the explanations for why the hot gas layer temperature and plume temperatures for the wall and corner configuration were lower than the calculated values, theoretical values and the results from older experiments. It is possible that heat energy was lost from the compartment through these cracks, however, no leakage was noticed during the experiment. The cracks could also have allowed more effective heating of the internal wall material local to the cracks, causing additional losses from conduction. The centre configuration did, however, match the theory and due to this fact, the cracks might not be the main error source or the effect of the cracks is proximity-based and the centre configuration is too far away from any cracks.

Figure 35: Crack above corner.

Figure 36: Crack in the back wall.

Figure 37: Crack below the room.

Figure 38: Crack in the corner where the burner was placed.

Figure 39: Crack inside the room.

Error sources in calculations are the ambient temperature T_a where the temperature inside the laboratory in which the experiment was conducted changed slightly over time during the tests. This should not cause a large difference but might change the result by a minuscule amount. Another variable that can cause a larger difference in the result is h_k in the MQH method, equation 9, which has been estimated from

a previous experiment conducted in the same compartment. This variable is time-dependent which can cause problems if the tests do not have the same duration and heat release rate affecting the compartment. The theoretically calculated value using material data is marginally different and does not cause a noticeable difference. However, while drastically changing h_k would change the relationship and improve between the MQH method and the experimental values by lowering the calculated hot gas layer temperature for the corner configuration to fit better with the modification factors from Mowrer and Williamson (1987) however the centre configuration would lose the perfectly aligned relationship between theoretical MQH and experimental data in the centre configuration. Meaning that rather than h_k being important it is more important to determine how and to which material properties that Mowrer and Williamson implemented in their experiment to determine their modification factors.

As seen in figure 34, the airflow could be a major error source for the hot gas layer temperature, where the hot gas layer loses the wall effect when the flame is pushed away from the wall. When this happens the flame rather resembles the flame from the centre configuration. The opening of the test room was always positioned toward the open door in the laboratory allowing the in-flow of air to flow straight into the test room. This might not have caused a problem for the corner configuration since it would have just been pushed into the corner. In hindsight, the test room could have been placed with its opening in the opposite direction to avoid this.

7 Conclusion

The results from the experiment conducted only partially correspond with theory and previous studies. In the results from the experiment conducted in this thesis, the hot gas layer temperature increased for fires in corners, just not as much as predicted by previous studies. The hot gas layer temperature did not increase for fires along walls, as opposed to what was predicted in theory and by comparing with results from Mowrer and Williamson (1987). From the results of the experiment of this thesis, it would be more reasonable to utilise 1.3 as the modification factor for the corner configuration and no modification factor for the wall configuration. The experiment proved to have many uncertainties and possible errors, which render the proposed modification factors unreliable and they need to be validated in further studies. The tests with liquid heptane gave an increased temperature for corner configuration compared to wall configuration. The centre configuration gave a higher heat release rate than predicted and is therefore not possible to use when compared to the wall and corner configuration.

Flame heights for the 5 and 10 kW tests did increase according to theory when using a modified flame height correlation. In the 20 kW fire, the flames were limited by the compartment size, and no conclusions could be made for that heat release rate due to the flames extending to the ceiling and spreading out horizontally under the ceiling. Flame height does not seem to differ depending on the fuel source, however, it should be noted that the sample size is small. Using the modified flame height correlation gave a better estimate of the flame height than the unmodified correlation.

Plume temperatures did give results with increasing temperatures for fires against walls and even further for fires in corners similar to the theory and proposed modification factors. The measurements of plume temperature are however very unreliable, which adds big uncertainty to the conclusions about plume temperature. Liquid heptane corresponds quite well with the results from gaseous propane for the wall and centre configuration. For the corner configuration, the plume temperatures are unreliable due to measurement errors. The equation used was also not valid for the corner configuration using 10 kW and 20 kW.

The simulations in FDS gave results that agreed fairly well with results from the hand calculations but did not correspond very well with the results from the experiment conducted in this thesis. The simulations did show an increase in hot gas layer temperature for both the wall and corner configuration compared to the centre configuration. From the results, the conclusion is that FDS can not be used to validate the experimental results of this thesis.

It was discussed how the material the compartment was constructed of contributed to the deviating results from theory and previous studies. The theory and modification factors for the MQH correlation proposed by Mowrer and Williamson (1987) that was used for calculating hot gas layer temperatures for fires in corners and along walls, was developed using only one size of compartment and only one type of material on the walls. Comparing the results from the experiment from this thesis with the results from the experiments conducted by McGrattan et al. (2018), both experiments resulted in no increase in hot gas layer temperature for the fire position flush to a wall. However, the results from McGrattan et al. did not display any increase in hot gas layer temperature for the corner fire, as opposed to the results from the experiment in this thesis.

7.1 Further research

Further experiments should be conducted using different materials and the same materials as this thesis but without damage to determine if the modification factors suggested by Mowrer and Williamson (1987) are dependent on the material of the compartment. Experiments comparing hot gas layer temperatures of both small-scale and full-scale are also of interest for further research. Differences in compartment size, heat release rate, and compartment materials are all variables that could be further researched to find if the wall configuration truly has an impact on the hot gas layer temperature. Since the flow of air from outside the laboratory into the test compartment might have influenced the wall configuration, airflow into the compartment should be considered in future studies.

More experiments should be made with measurements on plume temperature for fires with different positions, and with good methods to make accurate readings of the plume temperature. For example stationary thermocouple trees, like the ones used by McGrattan et al. (2018). As well as visual recording equipment which can show when and if measurements are taken in the flames instead of the plume.

Differences in hot gas layer temperatures between different versions of FDS should be further studied to determine how the changes between the versions cause the difference and to which extent these changes are realistic or not.

While the wall configuration did not attribute to a higher hot gas layer temperature, the corner configuration certainly did. With this information and the data from previous studies, ways to implement building design measures and other countermeasures to limit the corner effect should be looked into.

References

Azhakesan, A., Shields, T., Silcock, G., & Quintiere, J. (2003). An Interrogation Of The MQH Correlation to Describe Centre And Near Corner Pool Fires. *Fire Safety Science*, *7*, 371–382. https://doi.org/10.3801/IAFSS.FSS.7-371

Babrauskas, V. (2016). Heat Release Rates. In *SFPE Handbook of Fire Protection Engineering*. Society of Fire Protection Engineers. https://doi.org/10.1007/978-1-4939-2565-0

BIV. (2013). *CFD-beräkningar med FDS*. Föreningen för brandteknisk ingenjörvetenskap.

Bruns, M. (2018). Estimating the Flashover Probability of Residential Fires Using Monte Carlo Simulations of the MQH Correlation. *Fire Technology*, *54*, 187–210. https://doi.org/10.1007/s10694-017-0680-0

Carmignani, L. (2021). Flame Tracker: An image analysis program to measure flame characteristics. *SoftwareX*, *15*. https://doi.org/10.1016/j.softx.2021.100791

Cox, G., & Kumar, S. (2002). Modelling Enclosure Fires Using CFD. In *SFPE Handbook of Fire Protection Engineering*. Society of Fire Protection Engineers. https://doi.org/10.1007/978-1-4939-2565-0

Deal, S., & Beyler, C. (1990). Correlating Preflashover Room Temperatures. *Journal of Fire Protection Engineering*, *2*(2), 33–48.

Dittmer, T., & Jämtäng, U. (2006). *Känslighetsanalys av FDS och dess undermodeller i ett tunnelscenario*. Department of Fire Safety Engineering, Lund University.

Drysdale, D. (2011). *An Introduction to Fire Dynamics*. Wiley.

Foote, K. L., Pagni, P., & Alvares, N. J. (1986). Temperature Correlations for Force-Ventilated Compartment Fires. *Fire Safety Science 1*, 139–148.

Hansen, R., & Ingason, H. (2010). *Model scale fire experiments in a model tunnel with wooden pallets at varying distances*. Mälardalens högskola.

Hasemi, Y., & Tokunaga, T. (1984). Flame Geometry Effects on the Buoyant Plumes from Turbulent Diffusion Flames. *Fire Science and Technology*, *4*(1), 15–26. https://doi.org/10.3210/fst.4.15

Heskestad, G. (1983). Virtual origins of fire plumes. *Fire Safety Journal*, *5*(2), 109–114. https://doi.org/10.1016/0379-7112(83)90003-6

Heskestad, G. (1984). Engineering relations for fire plumes. *Fire Safety Journal*, *7*(1), 25–32. https://doi.org/10.1016/0379-7112(84)90005-5

Heskestad, G. (1995). Fire Plumes. In *SFPE Handbook of Fire Protection Engineering*. Society of Fire Protection Engineers. https://doi.org/10.1007/978-1-4939-2565-0

K. Sharma, P., Gera, B., & Singh, R. K. (2010). A CFD Validation of Fire Dynamics Simulator for Corner Fire. *CFD Letters*, *2*(4), 137–148. https://www.akademiabaru.com/submit/index.php/cfdl/article/view/3510

Karlsson, B., & Quintiere, J. G. (2022). *Enclosure Fire Dynamics* (N. Johansson, Ed.). CRC Press.

Lattimer, B. Y., & Sorathia, U. (2003). Thermal characteristics of fires in a noncombustible corner. *Fire Safety Journal*, *38*(8), 709–745. https://doi.org/10.1016/S0379-7112(03)00065-1

Ma, T., & Quintiere, J. (2003). Numerical simulation of axi-symmetric fire plumes: accuracy and limitations. *Fire Safety Journal*, *38*(5), 467–492. https://doi.org/10.1016/S0379-7112(02)00082-6

McCaffrey, B. J., Quintiere, J. G., & Harkleroad, M. F. (1981). Estimating Room Temperatures and the Likelihood of Flashover Using Fire Test Data Correlations. *Fire Technology*, *17*(2), 98–119.

McGrattan, K., Selepak, M., & Hnetkovsky, E. (2018). *Estimating Room Temperatures from Fires along Walls and in Corners*. National Institute of Standards; Technology.

McGrattan, K., Hostikka, S., Floyd, J., McDermott, R., & Vanella, M. (2021a). Fire Dynamics Simulator Technical Reference Guide Volume 3: Validation, NIST Special Publication 1018-3 (6th ed.). https://doi.org/10.6028/NIST.SP.1018

McGrattan, K., Hostikka, S., Floyd, J., McDermott, R., & Vanella, M. (2021b). Fire Dynamics Simulator User's Guide, NIST Special Publication 1019 (6th ed.). https://doi.org/10.6028/NIST.SP.1019

McGrattan, K., McDermott, R., Weinschenk, C., & Forney, G. (2013). Fire Dynamics Simulator, Technical Reference Guide, Sixth Edition. https://doi.org/10.6028/NIST.sp.1018

Mowrer, F., & Williamson, R. (1987). The influence of Walls, Corners and Enclosures on Fire Plumes. *Fire Technology, vol. 23*, 133–145.

MSB, Myndigheten för samhällsskydd och beredskap. (2022). IDA Fire data from Swedish fire brigade. Retrieved September 28, 2022, from https://ida.msb.se/ida2#page=a73f6dc8-8956-491d-a7ec-3b521a8a0c8d

Nystedt, F., & Frantzich, H. (2011). *Kvalitetsmanual för brandtekniska analyser vid svenska kärntekniska anläggningar*. Lunds Tekniska Högskola, Division for Fire Safety Engineering.

Quintiere, J. G., Steckler, K., & Corley, D. (1984). An Assessment of Fire Induced Flows in Compartments. *Fire Science and Technology*, *4*(1), 1–14. https://doi.org/10.3210/fst.4.1

Takahashi, W., Sugawa, O., Tanaka, H., & Ohtake, M. (1997). Flame And Plume Behavior In And Near A Corner Of Walls. *Fire Safety Science*, *5*, 261–271. https://doi.org/10.3801/IAFSS.FSS.5-261

Webb, A., Dowling, V., & McArthur, N. (1999). *Fire performances of materials*. CSIRO Fire Science; Technology Laboratory.

Yunlong, L., & Vivek, A. (2004). *Evaluation of Phoenics CFD Fire Model Against Room Corner Fire Experiments*. CSIRO Fire Science; Technology Laboratory.

Zeinali, D. (2019). *Flame Spread and Fire Behaviour in a Corner Configuration*. Ghent University.

Zukoski, E. (1995). *Properties of Fire Plumes*. Academic Press.

Zukoski, E., Kubota, T., & Cetegen, B. (1980). *Entrainment in Fire Plumes* (Vol. 39).

Appendix 1 - Mesh sensitivity analysis

The mesh sensitivity analysis is presented in figures 40, 41 and 42. The dashed line represents the average hot gas layer temperature from the simulations with 1 cm mesh, and the full line represents the average hot gas layer temperatures from the simulations with 2 cm mesh. The average hot gas layer temperatures are calculated as described in section 4.2.5. The 1 cm simulations were simulated in FDS version 6.7.7, while the 2 cm simulations were simulated in FDS version 6.7.9.

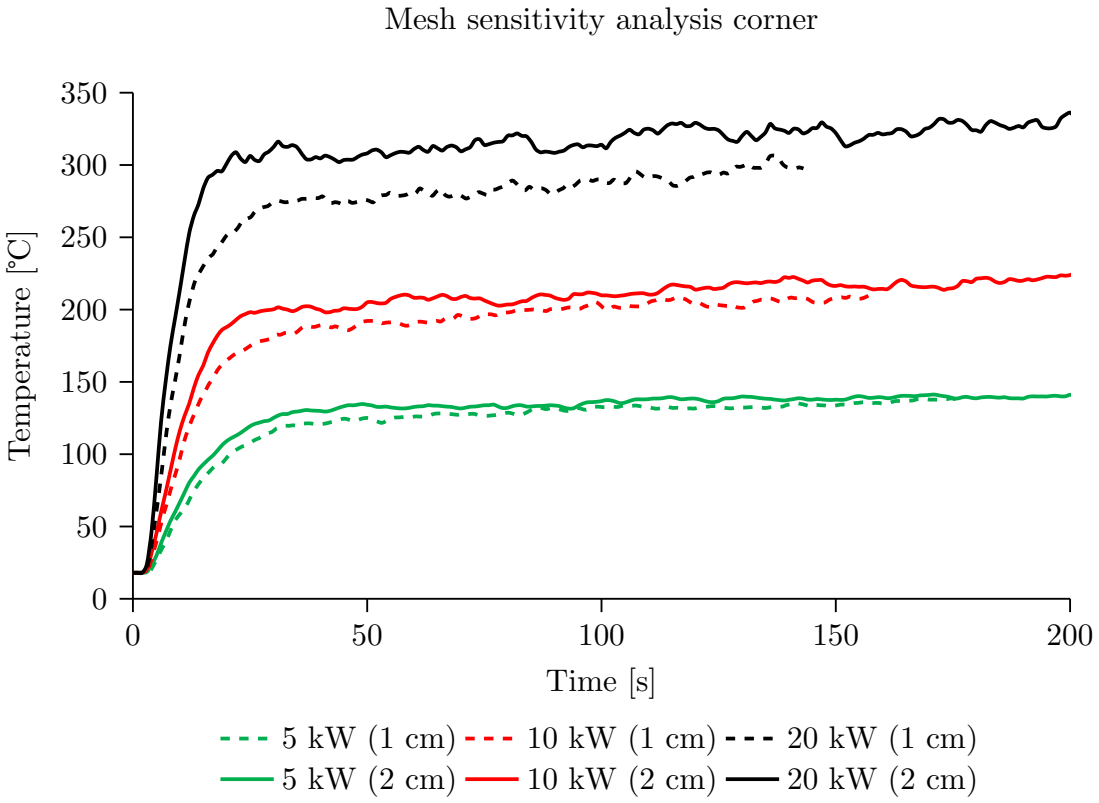

Figure 40: Difference in average hot gas layer temperature between 1 cm mesh and 2 cm mesh for corner position simulation.

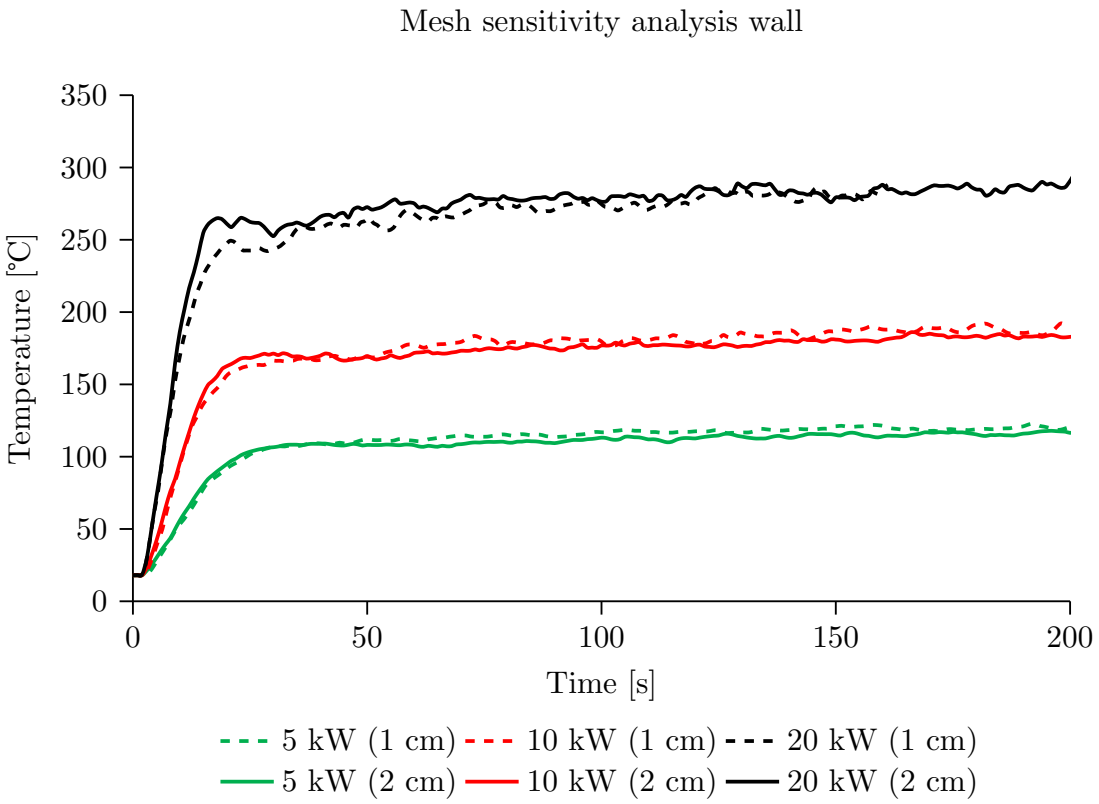

Figure 41: Difference in average hot gas layer temperature between 1 cm mesh and 2 cm mesh for wall position simulation.

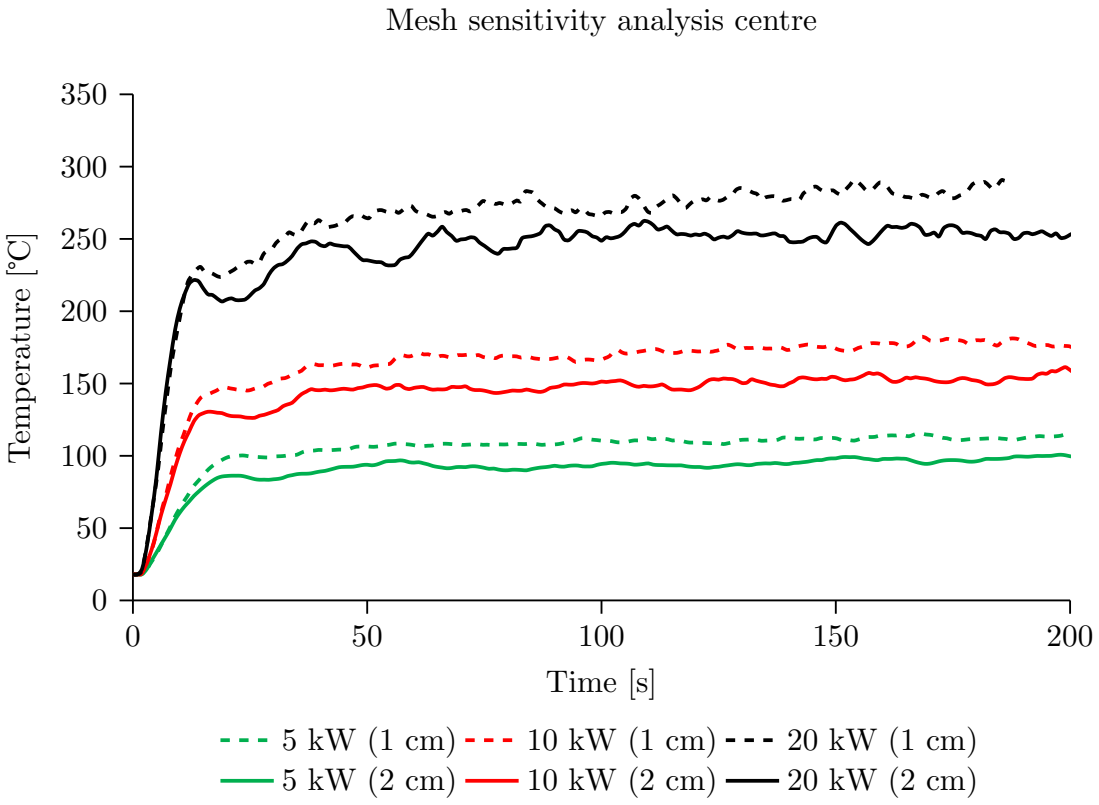

Figure 42: Difference in average hot gas layer temperature between 1 cm mesh and 2 cm mesh for centre position simulation.

As seen in the above figures, the difference between the 1 cm and 2 cm mesh resolutions varies depending on the heat release rate and position of the fire. Despite all values not being on par with each other, a reasonable agreement between the mesh resolutions can be seen, especially in the trends of the different results.

Appendix 2 - FDS code

This appendix contains the code for one of the simulations in FDS, the 10 kW corner fire. The only difference between the different heat release rates and positions of the fires is the position of some of the devices and slice files, as well as the heat release rate per unit area for 'Surface02'.

```
Corner_10_small.fds
Generated by PyroSim - Version 2021.4.1201
Oct 26, 2022 1:13:37 PM

&HEAD CHID='Corner_10_small', TITLE='Corner_10_small'/
&TIME T_END=900.0/
&DUMP DT_DEVC=1.0, DT_HRR=1.0, DT_SLCF=1.0, DT_SL3D=2.0,
   SMOKE3D=.FALSE./
&MISC TMPA=18.0/

&MESH ID='MESH', IJK=44,87,44, XB
   =-0.04,0.84,-0.5,1.24,-0.04,0.84/


&REAC ID='Propane',
      FUEL='PROPANE',
      CO_YIELD=5.0E-3,
      SOOT_YIELD=0.024,
      HEAT_OF_COMBUSTION=4.41E+4,
      RADIATIVE_FRACTION=0.25/

&DEVC ID='201', QUANTITY='THERMOCOUPLE', XYZ
   =0.725,0.105,0.785/
&DEVC ID='202', QUANTITY='THERMOCOUPLE', XYZ
   =0.725,0.105,0.74/
&DEVC ID='203', QUANTITY='THERMOCOUPLE', XYZ
   =0.725,0.105,0.62/
&DEVC ID='204', QUANTITY='THERMOCOUPLE', XYZ
   =0.725,0.105,0.56/
&DEVC ID='205', QUANTITY='THERMOCOUPLE', XYZ
   =0.725,0.105,0.5/
&DEVC ID='206', QUANTITY='THERMOCOUPLE', XYZ
   =0.725,0.105,0.44/
&DEVC ID='207', QUANTITY='THERMOCOUPLE', XYZ
   =0.725,0.105,0.32/
&DEVC ID='208', QUANTITY='THERMOCOUPLE', XYZ
   =0.725,0.105,0.14/
&DEVC ID='209', QUANTITY='THERMOCOUPLE', XYZ
   =0.445,-0.015,0.615/
&DEVC ID='210', QUANTITY='THERMOCOUPLE', XYZ
   =0.445,-0.015,0.565/
```

```
&DEVC ID='211', QUANTITY='THERMOCOUPLE', XYZ
   =0.445,-0.015,0.515/
&DEVC ID='212', QUANTITY='THERMOCOUPLE', XYZ
   =0.445,-0.015,0.465/
&DEVC ID='213', QUANTITY='PRESSURE', XYZ=0.445,-0.015,0.615/
&DEVC ID='214', QUANTITY='PRESSURE', XYZ=0.445,-0.015,0.565/
&DEVC ID='215', QUANTITY='PRESSURE', XYZ=0.445,-0.015,0.515/
&DEVC ID='216', QUANTITY='PRESSURE', XYZ=0.445,-0.015,0.465/
&DEVC ID='205dP', QUANTITY='PRESSURE', XYZ
   =0.445,-0.015,0.505/
&DEVC ID='206dP', QUANTITY='PRESSURE', XYZ
   =0.445,-0.015,0.44/
&DEVC ID='207dP', QUANTITY='PRESSURE', XYZ
   =0.445,-0.015,0.32/
&DEVC ID='208dP', QUANTITY='PRESSURE', XYZ
   =0.445,-0.015,0.14/
&DEVC ID='201_T', QUANTITY='TEMPERATURE', XYZ
   =0.725,0.105,0.785/
&DEVC ID='202_T', QUANTITY='TEMPERATURE', XYZ
   =0.725,0.105,0.74/
&DEVC ID='203_T', QUANTITY='TEMPERATURE', XYZ
   =0.725,0.105,0.62/
&DEVC ID='204_T', QUANTITY='TEMPERATURE', XYZ
   =0.725,0.105,0.56/
&DEVC ID='205_T', QUANTITY='TEMPERATURE', XYZ
   =0.725,0.105,0.5/
&DEVC ID='206_T', QUANTITY='TEMPERATURE', XYZ
   =0.725,0.105,0.44/
&DEVC ID='207_T', QUANTITY='TEMPERATURE', XYZ
   =0.725,0.105,0.32/
&DEVC ID='208_T', QUANTITY='TEMPERATURE', XYZ
   =0.725,0.105,0.14/
&DEVC ID='209_T', QUANTITY='TEMPERATURE', XYZ
   =0.445,-0.015,0.615/
&DEVC ID='210_T', QUANTITY='TEMPERATURE', XYZ
   =0.445,-0.015,0.565/
&DEVC ID='211_T', QUANTITY='TEMPERATURE', XYZ
   =0.445,-0.015,0.515/
&DEVC ID='212_T', QUANTITY='TEMPERATURE', XYZ
   =0.445,-0.015,0.465/
&DEVC ID='20101', QUANTITY='TEMPERATURE', XYZ
   =0.055,1.155,0.785/
&DEVC ID='20201', QUANTITY='TEMPERATURE', XYZ
   =0.055,1.155,0.74/
&DEVC ID='20301', QUANTITY='TEMPERATURE', XYZ
   =0.055,1.155,0.62/
&DEVC ID='20401', QUANTITY='TEMPERATURE', XYZ
   =0.055,1.155,0.56/
```

```
&DEVC ID='20501', QUANTITY='TEMPERATURE', XYZ
   =0.055,1.155,0.5/
&DEVC ID='20601', QUANTITY='TEMPERATURE', XYZ
   =0.055,1.155,0.44/
&DEVC ID='20701', QUANTITY='TEMPERATURE', XYZ
   =0.055,1.155,0.32/
&DEVC ID='20801', QUANTITY='TEMPERATURE', XYZ
   =0.055,1.155,0.14/
&DEVC ID='LAYER->HEIGHT', QUANTITY='LAYER HEIGHT', XB
   =0.405,0.405,0.355,0.355,0.0,0.8/
&DEVC ID='LAYER->LTEMP', QUANTITY='LOWER TEMPERATURE', XB
   =0.405,0.405,0.355,0.355,0.0,0.8/
&DEVC ID='LAYER->UTEMP', QUANTITY='UPPER TEMPERATURE', XB
   =0.405,0.405,0.355,0.355,0.0,0.8/
&DEVC ID='LAYERTT->HEIGHT', QUANTITY='LAYER HEIGHT', XB
   =0.725,0.725,0.105,0.105,0.0,0.8/
&DEVC ID='LAYERTT->LTEMP', QUANTITY='LOWER TEMPERATURE', XB
   =0.725,0.725,0.105,0.105,0.0,0.8/
&DEVC ID='LAYERTT->UTEMP', QUANTITY='UPPER TEMPERATURE', XB
   =0.725,0.725,0.105,0.105,0.0,0.8/
&DEVC ID='FLOW', QUANTITY='MASS FLUX Y', XB
   =0.29,0.59,-0.014,-0.014,0.0,0.65, SPATIAL_STATISTIC='
   AREA INTEGRAL'/
&DEVC ID='FLOW+', QUANTITY='MASS FLUX Y', XB
   =0.29,0.59,-0.014,-0.014,0.0,0.65, SPATIAL_STATISTIC='
   AREA INTEGRAL', QUANTITY_RANGE(1)=0/
&DEVC ID='FLOW-', QUANTITY='MASS FLUX Y', XB
   =0.29,0.59,-0.014,-0.014,0.0,0.65, SPATIAL_STATISTIC='
   AREA INTEGRAL', QUANTITY_RANGE(2)=0/

&MATL ID='Material01',
      SPECIFIC_HEAT=1.13,
      CONDUCTIVITY=0.175,
      DENSITY=870.0/

&SURF ID='Surface01',
      RGB=194,236,157,
      BACKING='VOID',
      MATL_ID(1,1)='Material01',
      MATL_MASS_FRACTION(1,1)=1.0,
      THICKNESS(1)=0.03/
&SURF ID='Surface02',
      COLOR='RED',
      HRRPUA=1000.0,
      TMP_FRONT=300.0/

&OBST ID='Floor', XB=-0.04,0.84,-0.04,1.24,-0.04,0.0,
   SURF_ID='Surface01'/
```

```
&OBST ID='Ceiling', XB=-0.04,0.84,-0.04,1.24,0.8,0.84,
   SURF_ID='Surface01'/
&OBST ID='Obstruction', XB=-0.04,0.84,-0.04,0.0,0.0,0.8,
   SURF_ID='Surface01'/
&OBST ID='Obstruction', XB=0.0,0.1,1.1,1.2,0.0,0.1, SURF_IDS
   ='Surface02','INERT','INERT'/
&OBST ID='Wall_inv', XB=-0.04,0.0,0.0,1.2,0.0,0.8, COLOR='
   INVISIBLE', SURF_ID='Surface01'/
&OBST ID='Wall', XB=-0.04,0.84,1.2,1.24,0.0,0.8, SURF_ID='
   Surface01'/
&OBST ID='Wall', XB=0.8,0.84,0.0,1.2,0.0,0.8, SURF_ID='
   Surface01'/

&HOLE ID='Hole', XB=0.29,0.59,-0.15,0.15,0.0,0.65/

&VENT ID='Mesh Vent: MESH [XMAX]', SURF_ID='OPEN', XB
   =0.84,0.84,-0.5,1.24,-0.04,0.84/
&VENT ID='Mesh Vent: MESH [XMIN]', SURF_ID='OPEN', XB
   =-0.04,-0.04,-0.5,1.24,-0.04,0.84/
&VENT ID='Mesh Vent: MESH [YMAX]', SURF_ID='OPEN', XB
   =-0.04,0.84,1.24,1.24,-0.04,0.84/
&VENT ID='Mesh Vent: MESH [YMIN]', SURF_ID='OPEN', XB
   =-0.04,0.84,-0.5,-0.5,-0.04,0.84/
&VENT ID='Mesh Vent: MESH [ZMAX]', SURF_ID='OPEN', XB
   =-0.04,0.84,-0.5,1.24,0.84,0.84/
&VENT ID='Mesh Vent: MESH [ZMIN]', SURF_ID='OPEN', XB
   =-0.04,0.84,-0.5,1.24,-0.04,-0.04/

&SLCF QUANTITY='TEMPERATURE', CELL_CENTERED=.TRUE., PBX
   =0.405/
&SLCF QUANTITY='TEMPERATURE', CELL_CENTERED=.TRUE., PBY
   =0.655/
&SLCF QUANTITY='TEMPERATURE', CELL_CENTERED=.TRUE., PBY
   =-0.015/
&SLCF QUANTITY='TEMPERATURE', CELL_CENTERED=.TRUE., PBX
   =0.055/
&SLCF QUANTITY='TEMPERATURE', CELL_CENTERED=.TRUE., PBY
   =1.155/
&SLCF QUANTITY='V-VELOCITY', VECTOR=.TRUE., CELL_CENTERED=.
   TRUE., PBY=-0.015/
&SLCF QUANTITY='VELOCITY', VECTOR=.TRUE., CELL_CENTERED=.
   TRUE., PBY=-0.015/
&SLCF QUANTITY='PRESSURE', CELL_CENTERED=.TRUE., PBY=-0.015/


&TAIL /
```